DESIGN OF AN IMPROVED D.C. HYSTERESIGRAPH

by

Richard G. Greb

Submitted in Partial Fulfillment of the Requirements

for the Degree of

Master of Science in Engineering

in the

Electrical Engineering

Program

Duane F. Rost Dec. 19, 1974

Adviser Date

Leon Rand 12-19-74

Dean of the Graduate School Date

YOUNGSTOWN STATE UNIVERSITY

March, 1975

ABSTRACT

DESIGN OF AN IMPROVED D.C. HYSTERESIGRAPH

Richard G. Greb

Master of Science in Engineering

Youngstown State University, 1975

A direct current hysteresigraph with digital display of peak magnetizing force, coercive force, peak induction and remanent induction was developed. The instrument provides measurement accuracy and simple operation not available with commercial equipment. Calibrated loop tracing is automatic, and a new form of electronic centering of the hysteresis loop simplifies loop tracing and improves measurement accuracy. The instrument is scaled for a 25 cm., 1000 turn Epstein frame.

TABLE OF CONTENTS

PAGE

CHAPTER I

INTRODUCTION

Hysteresis Loops

When a ferromagnetic material is magnetized in a cyclic magnetic field, a non-linear, irreversible relationship between the material induction B, and the applied field H, called a hysteresis loop results; having a typical shape shown in figure 1. The peak values of induction and field strength attained will be called B_m and H_m respectively. The induction remaining in the material when the field strength has gone to zero is called the remanent induction B_r, and the value of field strength required to drive the induction to zero is called the coercive force H_c. The cgs system of units with induction expressed in gausses and field strength expressed in oersteds will be used here since it is the most widely accepted system for magnetic measurements in this country.

The magnetization characteristics of a material are described by the material's hysteresis loop, but only at the particular frequency of excitation. The most notable effect on the shape of the hysteresis loop as the frequency increases, is the increase of loop area. The loop area is proportional to the energy dissipated in the material per cycle, and at low frequencies essentially d.c. the energy dissipated is called hysteresis loss. At higher frequencies the total loss is considered to be the sum of eddy current and d.c. hysteresis losses. Eddy current loss is caused by circulating electric currents generated within the (conductive) magnetic material by the changing magnetic field. This division of losses is a simplification which is no longer accepted in the classical manner[1], and is described to emphasisize the frequency dependence of the hysteresis loop.

Hysteresis Loop Measurement By The Ballistic Method

The d.c. hysteresis loops of magnetic materials have long been obtained by the so-called ballistic method, using circuits similar to the one shown in figure 2. The permeameter is constructed so that the field strength can be computed from the current I; and resulting changes in sample induction produce an induced voltage in the B-coil. Complete reversals or changes in the magnitude of I are obtained by operation of switches S_1 or S_2. The ballistic galvanometer G measures the change of induction after switch operation, since its deflection is proportional to the time integral of induced voltage. A minimum of instrumentation is required for this manual point by point method, but the required test procedure is time consuming and involves a certain amount of operator skill[2].

---

[1] B. D. Cullity, Introduction to Magnetic Materials (Reading, Mass.: Addison-Wesley, 1972), p.504.

[2] ASTM Special Publication 371-S1, Direct Current Magnetic Measurements for Soft Magnetic Material (Philadelphia: American Society for Testing and Materials, 1970), p.23.

A number of permeameters have been developed for the ballistic circuit[3, 4,5], the primary design considerations being production of a uniform field in the specimen and accurate determination of field strength.

A nearly ideal test arrangement is obtained with a toroidal or ring specimen having a B-coil uniformly wound over the specimen and an H-coil uniformly wound over the B-coil. The field strength can be accurately calculated from the exciting current in the H-coil using the well known formula;

$$H = .4\pi NI/L. \tag{1}$$

where H = field strength in oersteds

N = number of turns in H-coil

I = current in H-coil in amperes

L = mean circumference of specimen in centimeters.

Correction formulas can be applied when the radial thickness of the toroid is not small compared to the toroid mean diameter[6].

The Epstein frame is useful for testing samples in the form of small strips. It is constructed as shown in figure 3, with permanent coils forming the four sides of a square, and specimen strips are loaded into the frame forming a square magnetic circuit with joints at each

---

[3]R. L. Sanford, "Performance of Fahy Simplex Permeameter," Journal of Research, National Bureau of Standards, Vol. 4 No. 5 (May 1930), 703.

[4]B. J. Babbitt, "An Improved Permeameter for Testing Magnet Steel," Journal of the Optical Society, Vol 17, (1928), 47.

[5]B. D. Smith, " A New Full Range Permeameter," General Electric Review, Vol 38, No. 11 (November 1935), 520.

[6]P. R. Bardell, Magnetic Materials in the Electric Industry (London: MacDonald & Co., 1955), p.126.

corner. The air gaps and flux paths in the corners result in a certain amount of uncertainty in determining the effective magnetic path length[7], however, for general comparative testing, the value of L used in equation(1) has been standardized by the American Society for Testing and Materials at 94 cm. for a 25 cm. Epstein frame[8].

Hysteresigraphs

Instruments which produce direct continuous plots of hysteresis curves are called hysteresigraphs. Hysteresigraphs provide continuous excitation of the specimen, generally at very low frequencies within the writing speed of mechanical X-Y plotters, but sampling techniques have been used to extend operating frequencies into the audio range.

The first really practical recording hysteresigraph was described by P.P. Cioffi[9]. In the Cioffi instrument a signal proportional to the flux in a sample was obtained using a modification of the Edgar photoelectric fluxmeter[10]. The flux sensing winding (B-coil) of a permeameter was connected in series with a modified ballistic galvanometer

---

[7] D. C. Dieterly, "D. C. Permeability Testing of Epstein Samples with Double-Lap Joints," ASTM Special Technical Publication No. 85, Symposium on Magnetic Testing (1949), p. 39.

[8] ASTM Part 8, Standard a596-69, Direct Current Magnetic Properties Using Ring Test Procedures and the Ballistic Methods (Philadelphia: American Society for Testing and Materials, 1973), p.131.

[9] P. P. Cioffi, "A Recording fluxmeter of High Accuracy and Sensitivity," The Review of Scientific Instruments Vol 21 (July 1950), 624.

[10] R.F. Edgar, Trans. AIEE Vo. 56, (1937) p.805.

and the secondary of a mutual inductor. Any change of flux in the sample caused a deflection of the galvanometer which was sensed by an arrangement of two photocells in a bridge circuit. The bridge circuit was connected to the grid of a triode amplifier causing a current flow in the primary of the mutual inductor, so that the induced voltage on the mutual inductor secondary just cancelled out the permeameter B-coil voltage. In this way the galvanometer was deflection nulled by feedback and the current in the primary of the mutual inductor was proportional to flux. This system reportedly had an accuracy of .5% and a drift of less than .1% over a five minute period. The drift resulted from thermal EMF's in the circuit and from mechanical vibrations which disturbed the galvanometer balance point.

In the early 1960's the availability of high performance operational amplifiers made it practical to measure flux with operational integrators. Mazzetti and Soardo developed an electronic hysteresigraph using an operational integrator which had a drift rate of about 1% over a 30 minute period, making it suitable for very slow loop rates[11]. An important feature of their instrument was that the magnetizing current was generated by a closed loop circuit rather than a low frequency open loop oscillator. This resulted in good magnetizing current symetry and made it possible to introduce feedback to control the rate of change of magnetizing force to keep dB/dt constant.

[11] P.Mazzetti and P. Soardo, "Electronic Hysteresigraph Holds dB/dt Constant," The Review of Scientific Instruments Vol.37 (May 1966), 548.

An alternative to use of operational integrators for flux measurement was proposed by E. G. DeMott.[12] In his method the flux voltage is digitized by a voltage-to-frequency (V-F) converter. The output of the V-F converter is a pulse train whose frequency is proportional to the input voltage. The pulses from the V-F converter are counted so that the total number of pulses is proportional to the integral of the input voltage in a given time interval. For bipolar operation the V-F converter must provide a code indicating the polarity of the input voltage; and the counter must be able to count up or count down according to the polarity of the input voltage. For X-Y plotting of loops, the Y axis voltage is obtained by converting the counter output back to an analog voltage with a digital to analog converter. DeMott extimates the maximum integration error of .35% after calibration; with most of the error arrising in V-F converter nonlinearity. Although DeMott claims the V-F converter and counter combination has zero drift, this can be achieved in practice only if the V-F converter has a biased zero frequency cutoff point, which will result in integration errors for small input signals. The V-F converter method of flux measurement is somewhat expensive to implement, but can be used to advantage in computerized measurement schemes.

H. Capptuller used a V-F converter for flux measurement in a set up which completely digitized test results.[13] Test data was recorded

---

[12] E. G. DeMott, Journal of Applied Physics Vol. 37 (1966), 1118.

[13] H. Capptuller, "Numeric and Graphic Recording of Magnetization curves by Means of Analog-Digital Techniques," IEEE Transactions on Magnetics, Vol. Mag-6 (June 1970), 263.

in binary code on a magnetic tape recorder or a tape puncher and later fed into a computer which manipulated the data. A computer print out was obtained containing field strength, induction, polarization, residual flux, coercive force, differential permeability, and maximum energy product. The rate of change of flux was held constant in loop tracing so as to obtain the highest accuracy from the V-F converter. This equipment was designed for testing hard magnetic materials. The general procedure for testing hard materials is to place the specimen between the poles of an electromagnet which is capable of very high fields. Specimen induction can be measured with a B-coil in the normal manner, but field strength is usually measured with a Hall element flux transducer placed adjacent to the specimen; since the magnetizing current of the electromagnet windings is not a linear function of the field strength between the pole pieces. Capptuller estimates the relative accuracy of flux measurement at .03%, and the errors of remanence and coercive force at .2%.

A. T. English developed an instrument for continuous recording of 60 Hz. B-H loop parameters[14]. This equipment used a zero-crossing detector and a sample-and-hold amplifier for continuous measurement of coercive force or remanence.

---

[14]A. T English, "Apparatus for Continuous Recording of Coercive Force, Maximum Magnetization, and Remanent Magnetization of Ferromagnetic Materials," The Review of Scientific Instruments, Vol. 39 (September 1968), 1346.

A highly developed 60 Hz. loop tracer using sampling techniques was described by A. Manly Jr.[15]. A motor driven phase shifter enabled all points of the 60 Hz. loop to be sampled for low frequency tracing on a X-Y plotter. Key parameters such as H_c and B_r were displayed on digital voltmeters.

Finally in a paper published in 1972, J. Lenaerts and M. Vanwormhoudt presented a low frequency hysteresigraph with a novel programing feature[16]. The magnetizing current generator was conceptually similar to the closed loop design of Mazzetti and Soardo, but modified so that different values of H maxima and minima could be preprogramed for up to 10 complete cycles.

Advantages of Author's Hysteresigraph

The hysteresigraph described in this thesis was developed in order to satisfy a number of requirements which could not be obtained with commercial units. The most important features required were:

1. Simple, fast operating procedure.
2. Direct measurement of maximum induction B_m, remanence B_r, maximum field strength H_m, and coercive force H_c.

As a result, with the present instrument a calibrated B-H loop can be traced, and measurements of B_m, B_r, H_m and H_c can be recorded in less than 5 minutes. With regard to accuracy, the following design objectives were established:

---

[15] W. A. Manly, Jr. " A 5.5 - KOE 60-Hz Magnetic Hysteresis Loop Tracer With Precise Digital Readout", IEEE Transactions on Magnetics, (September 1971), 442.

[16] J. Lenaerts and M. Vanwarmhoudt, "A Practical Low Frequency Hysteresigraph," Journal of Physics Vol. 5 (1972), 560.

1. Automatic bipolar magnetizing current sweeping with positive and negative symmetry better than .1%.
2. Measurement of H_m to an accuracy of $\pm$ .25%.
3. Measurement of H_c to an accuracy of $\pm$ .5%.
4. Automatic centering of offset induction values to an accuracy of .1%.
5. Measurement of B_m to an accuracy of $\pm$ .25%.
6. Measurement of B_r to an accuracy of $\pm$ .5%.

All measurements displayed on the digital voltmeter are in engineering units of either kilogausses or oersteds, and the analog outputs for X-Y plotting are conveniently scaled for calibrated loop tracing.

The instrument was specifically designed for use with a 25 cm. Epstein frame, but ring core samples can be tested by application of appropriate correction factors. Computation of induction is derived from the value of an input potentiometer which is set to the sample weight in grams. The peak magnetizing force can be set to fixed values of 1 or 10 Oe., or to intermediate values of peak magnetizing force or resulting peak induction by a simple adjustment procedure.

An entirely new concept developed is automatic centering of the loop on the B-axis through electronic compensation. Loops are automatically centered about zero voltage by pressing a button on the control panel after one complete peak-to-peak flux excursion has occured. Automatic centering eliminates the effects of integrator drift for long sequential measurements, improves measurement accuracy, and in general simplifies recording of loops.

CHAPTER II

General Circuit Description

The instrumentation for recording hysteresis loops can be thought of as a specialized analog computer network. The B-coil of the permeameter (Epstein frame) provides a voltage which is proportional to the rate of change of flux enclosed; which must be integrated and multiplied by a constant to yield an output voltage proportional to flux density or induction. The magnetizing current is converted to a voltage and multiplied by a constant to provide a second output voltage proportional to field strength.

In order to provide symetry in magnetizing current, and to measure B_m, B_r, H_m, and H_c, certain switching operations must be combined with the computational circuitry above. All of these functions are realized by both linear and non-linear operational amplifier feedback networks. This approach results in highly stable and predictable circuit performance as will be shown later.

The block diagram of figure 4 will be used in the following general description of the operation of the B-H meter, and the complete circuit diagram is shown in figure 6.

The voltage e_1 at the B-coil terminals is integrated by an operational integrator whose output e_2 is a voltage proportional to the change of flux in the sample. The centering circuit adds a compensating voltage to e_2 if necessary so that the absolute values of the positive and negative peaks of e_2 are equal. Then the centered voltage

e_3 is multiplied by an amount determined by the sample weight potentiometer P1, so that the induction output signal e_4 is scaled to 1 volt per 10 kilogausses in the sample. The magnetizing current I_p in the H-coil produces a voltage drop e_5 across one of the shunt resistors for scaling. This voltage is then multiplied by a fixed constant yielding the magnetizing force output voltage e_6, which is equal to either 1 or 10 volts per oersted. The B and H output signals (e_4 and e_6) can be connected to an X-Y plotter for hysteresis loop tracing.

A full wave rectifier computes the absolute value of e_6 which becomes the input voltage to a comparator. When the absolute value of e_6 is equal to a reference voltage e_8, the comparator output provides a trigger pulse which causes a bistable multivibrator to change state. This effectively reverses the polarity of the constant input voltage to the current sweep integrator, whose output e_{11} is a triangular waveform with precise symetry. A feedback signal from the flux integrator can be summed at the input of the current sweep integrator in order to limit or reduce the slope of the magnetizing current ramp and thereby reduce dB/dt. The power amplifier has sufficient output current capability to drive the H-coil of the Epstein frame.

A zero crossing detector controls the operating mode of a sample and hold amplifier for measurement of B_m, B_r, H_m and H_c on the digital voltmeter. For measurement of B_m and H_m the biased output of the multivibrator is switched into the zero crossing detector so that the sample and hold amplifier goes into the hold mode at the point of maximum current in the H-coil. To measure B_r the H signal is switched into the zero crossing detector with the B signal being sampled. To measure H_c the B signal is switched into the zero crossing detector while the H signal is being sampled. A typical waveform and timing diagram is shown in figure 5.

The B-H meter is scaled for a 1000 turn, 25 cm. Epstein frame, and a peak magnetizing force of 10 oersteds. Up to 1 kilogram of steel can be loaded into the Epstein frame. A variable 60 Hz supply is built into the equipment for demagnetizing the steel before testing.

B and H Computing Circuits

Circuit Descriptions

In the following sections the various functional circuit blocks of the B-H meter will be described. Subscripted voltages and circuit components in the functional circuit block figures are the same as used in the complete circuit diagram of figure 6 unless otherwise stated.

B-Coil Integrator

According to Faraday's law, the voltage induced on a search coil of N turns surrounding the sample is proportional to the time rate of change of flux linking the coil.

$$e = N\,10^{-8}\ d\phi/dt \tag{2}$$

and

$$\int_{t_1}^{t_2} e\,dt = N\,10^{-8}\ (\phi_{t2} - \phi_{t1})\ \text{maxwells}\,. \tag{3}$$

Prior to development of electronic integrators, ballistic galvanometers were almost exclusively used to measure the above voltage integral (and are still widely used today), but ballistic galvanometers require a voltage pulse of very short duration compared to the galvanometer period for true integration, and do not provide an analog output signal.

High gain operational amplifiers with low drift can be used to provide nearly ideal integration of voltage. In figure 7 the operational integrator is shown. The input offset voltage e_{os} and the input bias current i_b of the operational amplifier are included since they are the largest source of integrator error at low frequencies. The circuit can be explained with the following analysis:

$$i_{in} = \frac{e_1 - e_{os}}{R_1}$$

$$i_c = i_{in} - i_b$$

$$e_2 = e_{os} - \frac{1}{C_1}\int i_c\, dt$$

thus $$e_2 = -\frac{1}{R_1C_1}\int e_1 dt + \frac{1}{R_1C_1}\int e_{os} dt + \frac{1}{C_1}\int i_b dt + e_{os}\,. \quad (4)$$

From equation (4) it is seen that the output voltage is the sum of the time integral of the input voltage, two terms which are time integrals of the offset voltage and bias current, and a constant term equal to the offset voltage. The constant offset voltage term is quite small and can be neglected, but the integrated offset voltage and bias current are drift terms which will increase with time causing a significant error. In a good quality chopper stabilized operational amplifier, e_{os} can be trimmed to less that 10^{-6} volt and i_b will be less than 10^{-10} ampere. In practice e_{os} is trimmed in polarity and magnitude to cause cancellation of drift terms. Unfortunately, both e_{os} and i_b will vary with temperature and age so that perfect drift cancellation can only be attained for a short period. The integrator used in the B-H meter has a typical drift of 10^{-5} volt per second for several hours after an e_{os} trim adjustment, and 10^{-4} volt per second for several weeks after a trim adjustment.

An additional source of drift results from leakage current through the shunt resistance of C_1. With a polystyrene capacitor this shunt resistance is typically 10^{12} ohms and for a capacitance of $.5 \times 10^{-6}$ farad the effective drift will be 2×10^{-6} volt per second for each volt of charge on C_1. The integrator is initially zeroed by discharging C_1 through the contacts of relay L_7.

Since the summing junction node S in figure 7 is at virtual ground, the input impedance of the integrator is equal to R_1. R_1 must be large enough to limit the current drawn from the B-coil, since any B-coil current would act in opposition to the H-coil current from which the magnetizing force is computed. The B-coil voltage will not exceed .05 volt even for fast loop rates, and the resulting current with a value of 5×10^4 ohm for R_1 is 10^{-6} ampere. The typical magnetizing current at H_c on the hysteresis loop (point of maximum rate of change of flux) is about 5×10^{-3} to 20×10^{-3} ampere, and therefore the actual magnetizing force calculated from the H-coil current could be low by no more than .02%; and less for slower loop rates where the B-coil voltage is less than .05 volt.

B Centering Circuit

If the steel sample is not perfectly demagnetized prior to loop tracing, the hysteresis loop will shift after the first few cycles by an amount equal to or somewhat less than the initial remanent flux. This shift causes the hysteresis loop to be offset from the electrical zero so that the flux integrator output e_2 will be proportional to the sample flux plus some uncertain d.c. component. Even if the steel is perfectly demagnetized prior to testing, some shift of the B-H loop will still occur, since a condition of cyclic symmetric magnetization doesn't exist until 2 or 3 magnetization cycles. The effect is exaggerated in figure 8, which shows the general trend in reaching a cyclically stable magnetization loop. When the peak magnetizing force is great enough to drive the material nearly into saturation, the shift is negligible. In addition to these magnetization effects, the voltage drift inherent in the operational amplifier integrator will result in an offset B-H loop. The electronic centering circuit described below senses the amount of loop offset and provides compensation to center the loop. This improves measurement accuracy and simplifies calibrated loop tracing.

The flux centering circuit consists of a positive peak detector (A_2,A_3), a negative peak detector (A_4,A_5), and a summing amplifier (A_6). The operation of the peak detectors will be discussed first. As shown in figure 9, a positive polarity input voltage applied to the non-inverting input of A_2 forces A_2 into positive saturation, and the diode D_1 is forward biased. Amplifier A_3 is connected inside the main feedback loop as an integrator, so that the output voltage e_{A3} is a ramp given by:

$$e_{A3} = -e_s t/R_4C_2 .$$

When e_{A3} is just greater than the input voltage e_2 (for $R_2 = R_3$), the output of A_2 goes negative and diode D_1 becomes reverse biased. With the input to the integrator effectively open circuited, the value of e_{A3} is held until a more positive input signal is applied, or until A_3 is reset by discharging C_2.

As shown earlier in the analysis of the flux integrator, the output of A_3 will be subject to input bias current and capacitor leakage drift. The offset voltage e_{os} of A_3 does not cause significant drift because the diode D_1 is reverse biased most of the time. The largest source of drift is actually low gain charging of the integrator from the voltage e_s through the finite reverse biased resistance of D_1. This drift is given by:

$$e_{A3 \text{ drift}} = -\frac{1}{(R_d+R_4)C_2}\int e_s dt \quad , \tag{5}$$

where R_d is the diode reverse biased resistance. Use of a second diode D_2 as shown in figure 10 can reduce drift by a factor of 1000 or more by isolating e_s. Then e_d becomes the voltage integrated in equation (5), rather than e_s; and e_d is quite small being the voltage drop across R_{33} caused by leakage current through R_d. Accuracy of peak measurement depends upon d.c. offsets at A_2, ratio matching of R_2 and R_3, and the circuit response time. In general, a certain amount of overshoot will occur for fast rise inputs, because when the output voltage e_{A3} just equals the input voltage e_2, it takes a finite time for A_2 to go out of positive saturation and during this time A_3 will continue to integrate. The amount of overshoot can be shown to be given by:

$$e_{A3 \text{ overshoot}} = \bar{e}_s \; t/R_4C_2 \quad , \tag{6}$$

where $\bar{e}_s$ is the average value of e_s during the transition, and t is the transition time. The overshoot can be reduced by increasing R_4C_4 at the expense of overall response time, but a response time of approximately one second works well for this slow application.

Negative peak detection is achieved by simply reversing the polarity of the diodes.

Flux centering results from summing 1/2 the output voltages of the positive and negative peak detectors with the voltage e_2 from the integrator, as shown in figure 11. In order to describe the centering operation more explicitly, let e_{pp} be the positive peak value of the integrator output e_2, and let e_{np} be the negative peak value of e_2. When the flux loop is not symmetrical in peak values, e_{pp} does not (4) equal e_{np}, and an offset term e_k can be defined;

$$e_k = \frac{e_{pp} + e_{np}}{2} , \tag{7}$$

so that if a voltage "$-e_k$" were added to the integrator output, the flux loop would be symmetrical about zero voltage. The peak detectors (5) provide a voltage twice this compensating value since they have gains of -1, and

$$e_{A3} = -e_{pp} \qquad e_{A5} = - e_{np} . \tag{8}$$

The required factor of 1/2 is obtained at the summing amplifier A_6 by choosing $R_9 = R_{10} = 2R_8$. The output of A_6 is then:

$$e_3 = -\left(\frac{e_{A3}}{2} + \frac{e_{A5}}{2} + e_2 \right) \tag{9}$$

and so $$e_3 = -(e_2 - e_k), \tag{10}$$

which is the desired result. Centering can only be achieved after the flux loop is stable. If, for example, after the positive and negative peaks are sensed, the loop undergoes additional positive drift, the new positive peak will be detected, but the new (reduced) negative peak will not be detected, and the converse is true for additional negative drift. In the former case, the negative peak detector must first be reset by discharging C_3. In practice, both peak detectors are simultaneously reset by energizing the contacts of relay L_8. By opening switch S_8 the peak detectors are connected to ground and the centering circuit is bypassed.

B-Scaling Amplifier

Amplifier A_7 is a simple inverter with a precision potentiometer input resistor, which is set to the sample weight in order to scale the output to 1 volt per 10 kilogausses of induction in the sample. The required gain of A_7 is calculated from the Epstein frame parameters and the flux integrator gain. First, combining equations (3) and (4), the output voltage e_3 of A_6 is:

$$
\begin{aligned}
e_3 &= -e_2 \text{ (centered)} \\
&= \frac{N \phi \, 10^{-8}}{R_1 C_1} \\
&= \frac{NAB \, 10^{-8}}{R_1 C_1} \qquad (11)
\end{aligned}
$$

where ϕ = sample flux in maxwells

N = number of turns in B-coil

A = sample cross sectional area in cm.^{2}

B = sample induction in gausses .

The cross sectional area of the sample can be derived from the sample weight and density as:

$$A = \frac{W}{4 \rho L_s} \qquad (12)$$

where W = total sample weight in grams

ρ = sample density in grams per cubic cm.

L_s = length of Epstein strips in cm.

The total sample weight is divided by 4 since there are four legs of assumed equal area laminations. Substituting equation 9 into equation 8 gives the output of A_6 in terms of sample weight and induction.

$$e_3 = \frac{NWB\ 10^{-8}}{4\rho R_1 C_1 L_s} \tag{13}$$

The desired result is to scale e_3 with amplifier A_7 so that the final output voltage e_4 is equal to 1 volt per 10 kilogausses induction in the sample.

$$\text{thus} \qquad e_4 = \frac{B}{10^4} \tag{14}$$

The gain of A_7 is just the ratio of the feedback resistor to the input resistor R_{12}/P_1 (with polarity inversion).

$$\text{thus} \qquad e_4 = -\frac{e_3\ R_{12}}{P_1}$$

$$= -\frac{NWBR_{12}\ 10^8}{4\rho R_1 C_1 L_s P_1} \tag{15}$$

Combining equations (14) and (15), and solving for the ratio R_{12}/P_1 the result is:

$$\frac{R_{12}}{P_1} = \frac{4\rho R_1 C_1 L_s\ 10^4}{NW} \ . \tag{16}$$

The value of ρ used in equation (16) was 7.65 g./cm.^{3} (most common density), and when samples of a different density are tested, a correction factor for the weight setting on P_1 shown below is required.

$$W_{corrected} = W_{actual} \frac{\rho}{7.65} \tag{17}$$

If the values of R_1 and C_1 are accurately known, then a convenient calibration procedure consists of developing a constant voltage e_3 by operating the B-H meter and then shorting the input terminals of the flux integrator. The ratio of e_4/e_3 is then measured with an accurate digital voltmeter while R_{12} is trimmed until the correct ratio according to equation (16) is obtained.

A more fundamental calibration procedure which does not require knowledge of precise circuit values (as would be the case months or years after assembly, because of component drift), consists of applying a precise voltage inpulse to the integrator and measuring the output voltage e_4. To calculate what e_4 should be for a given input pulse and sample weight setting on P_1, a gain factor K_B for the entire B computing circuit will be derived;

$$e_4 = K_B \int e_1 dt = \frac{B}{10^4} , \tag{18}$$

and equation (2) can be rewritten as:

$$e_1 = \frac{NW\ 10^{-8}}{4 \rho L_s} \frac{dB}{dt} , \tag{19}$$

then solving for K_B ;

$$K_B = \frac{4 \rho L_s 10^4}{NW} . \tag{20}$$

If a constant voltage e_1 is applied to the input of the flux integrator for a time t seconds, the integrated and amplified voltage e_4 should then be:

$$e_4 = K_B \int e_1 dt = K_B e_1 t$$

$$= \frac{4 \rho L_s 10^4}{NW} e_1 t \quad . \tag{21}$$

Getting back to the operation of the B-H meter, the voltage e_4 which is proportional to sample induction is continuously displayed on the analog meter M_1 and can be used to drive the Y axis of an X-Y plotter for loop tracing. It is also either displayed on the digital meter or used as an input to the zero crossing detector.

H-Scaling Amplifier

The magnetic field strength inside a uniformly wound toroid is again:

$$H = \frac{.4\pi NI}{L_c} \text{ oersteds} \tag{22}$$

where I = current in winding in amperes

N = number of turns in winding

L_c = mean magnetic path length in centimeters

For an Epstein frame the mean path length is not equal to the geometric mean path length because of uncertain flux distributions and air gaps in the joints, but it is common to use 94 cm. as the mean path for 25 cm. frames. With 1000 turns, the required current for a 1 oersted field strength is then:

$$I_{H1} = \frac{HL_c}{.4\pi N}$$

$$= \frac{94}{.4\,\pi\,10^3}$$

$$= .0748 \quad \text{ampere} \quad ,$$

and $I_{H10} = .748$ ampere .

A shunt resistor either R_{13} or R_{14} is used to measure the magnitude of the magnetizing current. Values of shunt resistors R_{13} and R_{14} providing a 1 volt drop for field strengths of 1 and 10 Oe. are calculated as:

$$R_{13} = 1 \text{ volt}/.0748 \text{ ampere}$$

$$= 13.368 \text{ ohm} \qquad (H_m = 1 \text{ Oe.}) \quad ,$$

$$\text{and} \quad R_{14} = 1.3368 \text{ ohm} \qquad (H_m = 10 \text{ Oe.}) \; .$$

The differential amplifier A_8 provides a voltage gain of 10 for the voltage across the shunt resistor. The input resistance of A_8 would have a nominal loading effect on R_{13} or R_{14}, and compensated values for these resistors must be calculated. In general, the input resistance of a balanced ($R_{18}/R_{15} = R_{17}/R_{16}$) differential amplifier depends on the potential at both the inverting and non-inverting inputs; but when the non-inverting input is close to signal ground or for large gains, the input resistance is nearly equal to the input resistor value $R_{15} = R_{16}$, or in this case 10^4 ohm. With an input resistance this high, the compensation required for R_{14} is less than .02% and was ignored, however, R_{13} is more significantly loaded by the 10^4 ohm parallel resistance of A_8. The compensated value of R_{13} is the value which in parallel with 10^4 ohm has an equivalent resistance of 13.368 ohm.

$$R_{13\,comp} = \frac{R_{13}\,10^4}{(10^4 - R_{13})} \tag{23}$$

$$= 13.381 \text{ ohm} \quad .$$

Amplifier A_8 is used in the differential mode since an ordinary inverter would amplify in addition to the drop across the shunt resistor, the small but significant drop in the leads from the shunt resistor to signal common.

By virtue of the gain of 10 of A_8, the output voltage e_6 is scaled to 10 volts per 1 oe. or 10 volts per 10 Oe. when R_{13} or R_{14} respectively are used. The field strength voltage e_6 is displayed on the analog meter M_2 and can be used to drive the X-axis of an X-Y plotter for loop tracing. It is also either displayed on the digital meter or used as an input to the zero crossing detector, and is an input signal to the full wave comparator described next.

Magnetizing Current Generator

Full Wave Comparator

The full wave comparator provides a trigger pulse when the absolute value of e_6 is just equal to a reference voltage; causing the magnetizing current to retrace. In order to simplify discussion of the operation of the full wave comparator, the conventional absolute value circuit will first be described using figure 12.

First, the amplifier A_9 is used as a precision limiter, that is:

$$\text{for } e_6 < 0 \quad \text{then } e_L = -e_6$$

$$e_6 > 0 \quad \text{then } e_L = 0 \ .$$

To see this result, note that for negative values of e_6 the output of A_9 is positive, and diode D_{14} is forward biased. As in the simple inverter, the summing junction S is at virtual ground.

$$i_1 = i_2 = \frac{e_6}{R_{19}} \ ,$$

and $\quad e_L = -i_2 R_{20} = -\dfrac{e_6 R_{20}}{R_{19}}$;

let $\quad \dfrac{R_{20}}{R_{19}} = 1$,

then $\quad e_L = -e_6 \qquad \text{for } e_6 < 0$. (24)

For positive values of e_6 the output of A_9 is negative and D_{14} is reverse biased so that:

$$i_2 = 0$$

and $\quad e_L = 0 \qquad \text{for } e_6 > 0$. (25)

Amplifier A_{10} is used as a summing inverter with two input resistors R_{21} and R_{22}.

$$i_3 = \frac{e_6}{R_{21}}$$

$$i_4 = \frac{e_L}{R_{22}}$$

$$i_5 = i_3 + i_4$$

then $\quad e_9 = -i_5 R_z$

$$= -\left[\frac{e_6}{R_{21}} + \frac{e_L}{R_{22}}\right] R_z \tag{26}$$

let $\quad R_{21} = R_z = 2R_{22}$

then substituting e_L from equations (24) and (25)

$$e_9 = -(e_6 - 2e_6) \qquad \text{for } e_6 < 0$$

$$= e_6 \tag{27}$$

and $\quad e_9 = -(e_6 - 0) \qquad \text{for } e_6 > 0$ (28)

therefore $\quad e_9 = -|e_6| \qquad \text{for all } e_6$. (29)

By adding a third input resistor R_{23} as shown in figure 13, and letting R_z become very large, A_{10} becomes a comparator. For this circuit equation (26) can be rewritten as:

$$e_9 = -\left[\frac{e_6}{R_{21}} + \frac{e_L}{R_{22}} + \frac{e_8}{R_{23}}\right] R_z \quad , \tag{30}$$

$$\text{and} \qquad e_9 = -\left[\frac{|e_6|}{R_{21}} + \frac{e_8}{R_{23}}\right] R_z \quad , \tag{31}$$

so that when $|e_6|$ is just greater than $e_8 R_{21}/R_{23}$ (which is negative in polarity), the output voltage e_9 goes negative. By substituting a zener diode Z_4 for R_z the output excursion of e_9 will be clamped to values compatible with the TTL gates of the bistable multivibrator which follows.

Bistable Multivibrator

Ordinarily a JK flip flop with triggering through the clock input would be a suitable bistable element. However, the output of the comparator may contain multiple pulses near the comparator trip point because of the slowly varying input signal (e_6). For this reason a special bistable circuit was designed with four NOR gates which responds to only the first falling edge of the comparator signal. When e_9 goes low the RC networks (C_8,R_{31} and C_9,R_{32}) effectively steer the input voltage e_9 to either gate 1 or gate 2. Gates 3 and 4 form an ordinary RS flip flop. The output of gate 3 can be set high initially by breaking the output of gate 2 to the input of gate 4, and this is done with relay L_1.

Sweep Integrator

The output of the bistable multivibrator is integrated in order to produce a linear sweep voltage for exciting the H-coil of the Epstein frame. Recalling the earlier analysis of operational integrators, the output of the current sweep integrator can be shown to be:

$$e_{11} = -\frac{1}{C_5}\int((e_{10}/R_{24}) - (15/R_{27}))dt \quad . \tag{32}$$

The reason for summing the multivibrator output e_{10} with the -15 volt reference is that e_{10} alone would only produce negative ramps since it is always positive. For equal positive and negative sweep speeds it is required that:

$$e_{10}/R_{24} = 15/R_{27}$$

$$\text{or} \quad R_{27} = 15R_{24}/4 \; , \tag{33}$$

where the nominal value of the flip flop voltage e_{10} is 4 volts in the high state. R_{27} is a variable resistor so that sweep rates can be manually balanced since e_{10} is not precisely specified by the manufacturer of the TTL gates.

Power Amplifier

The power amplifier is an inverter with adjustable gain set by front panel potentiometer P_2 so that the rate of loop tracing may be varied from about .1 to .005 Hz. The nominal sweep rate will be reduced by the dB/dt limiting described later. Without feedback the sweep rate can be calculated from the power amplifier A_{12} gain as follows. First, the self inductance of the primary winding can be neglected so that:

$$\frac{dI_p}{dt} = \frac{1}{R_p}\frac{de_{12}}{dt} \tag{34}$$

where I_p = H-coil magnetizing current in amperes

e_{12} = output voltage of power amplifier

R_p = combined resistance of primary winding and shunt resistor R_{13} or R_{14} in ohms .

The power amplifier is an inverter and:

$$e_{12} = -\frac{e_{11} R_{26}}{R_{25} + P_2} \; . \tag{35}$$

The sweep integrator voltage e_{11} can be approximated by

$$e_{11} \approx \frac{\pm 1}{C_5 R_{24}} \int 2dt \; . \tag{36}$$

Using equations (35) and (36), equation (34) can then be written as:

$$\frac{dI_p}{dt} = \frac{2 R_{26}}{(R_{25} + P_2)R_{24}C_5R_p} \quad \text{amperes per second .} \tag{37}$$

The only components in equation (37) which are not constant are P_2 and R_p. R_p is the total H-coil circuit resistance and depends on the maximum magnetizing force range as selected by S_2 (selecting R_{13} or R_{14}); the varation of R_p has the beneficial feature of helping to keep the loop frequency constant independent of maximum magnetizing force range.

dB/dt Feedback

It is desireable to keep dB/dt in the specimen small for two reasons. First, large dB/dt causes eddy currents in the specimen; changing the shape of the hysteresis loop so that the area HdB increases.

Also, as will be shown later, the sampling errors in measurement of H_m, H_c, B_m, and B_r are reduced as dB/dt and dH/dt are reduced. It is not convenient to simply have long loop tracing times, and a good compromise is to use feedback which reduces dH/dt in proportion to dB/dt. This can be achieved by connecting a capacitor C_4 between the output of the flux integrator A_1 and the inverting input of the current sweep integrator A_{11}, as shown in figure 14. It will be useful to show how the component values control the amount of feedback, and a convenient starting point for the circuit analysis is an equation giving the output voltage e_{11} of A_{11}.

$$e_{11} = -\frac{1}{C_5}\int i_{C5}dt$$

$$= -\frac{1}{C_5}\int (de_2/dt)C_4 dt \pm \frac{1}{C_5 R_{24}}\int 2dt \qquad (38)$$

and $$\frac{de_{11}}{dt} = -\frac{C_4}{C_5}\frac{de_2}{dt} \pm \frac{2}{C_5 R_{24}}. \qquad (39)$$

The first term on the right side of equation (39) is proportional to the rate of change of flux in the specimen, and the second term is proportional to the "biased" multivibrator output. Equation (39) shows that when the signs of the two terms on the right are opposite (condition of negative feedback), then the rate of change of e_{11} will be reduced by an amount proportional to the rate of change of flux.

To carry the analysis further, a few constants will be defined. Let K_1 give the relationship between the voltage e_2 and the flux density of the specimen.

$$e_2 = K_1 B$$

then $$\frac{de_2}{dt} = K_1\frac{dB}{dt}$$

and $$K_1 = NA10^{-8}/R_1C_1 \text{ volts per gauss} . \tag{40}$$

Next let K_2 give the relationship between the output voltage of A_{11} and the magnetizing force.

$$e_{11} = K_2 H$$

then $$\frac{de_{11}}{dt} = K_2 \frac{dH}{dt} \tag{41}$$

and $$K_2 = \frac{L_c(R_{25} + P_2)R_p}{.4\pi NR_{26}} .$$

An incremental permeability μ_i will be difined as:

$$\mu_i = \frac{dB}{dH} . \tag{42}$$

Now using equations (40), (41), and (42), equation (39) can be rewritten as:

$$K_2 \frac{dH}{dt} = -\frac{C_4K_1}{C_5} \frac{dB}{dt} \pm \frac{2}{C_5R_{24}} \tag{43}$$

$$= \frac{K_2 dB}{\mu_i dt} .$$

Finally, if equation (43) is solved for dB/dt the result can be shown to be:

$$\frac{dB}{dt} = \pm \frac{2}{C_5R_{24}} \left[\frac{1}{\frac{K_2}{\mu_i} + \frac{C_4K_1}{C_5}} \right] . \tag{44}$$

Equation (44) can be used to calculate the circuit response or component sensitivity, but is somewhat complicated. In practice, all circuit values except C_4 were chosen from other constraints, and different values of C_4 were tried on a trial and error basis to give reasonable feedback or a fairly constant pen velocity when plotting. It is interesting that dB/dt can actually be kept constant if $K_2/\mu_i << C_4K_1/C_5$, since μ_i is the only term which is not constant.

The B-coil voltage e_1 could be used as a feedback signal directly into A_{11} through a resistor, since e_1 is proportional to dB/dt. However, the required low value of feedback resistance would load the B-coil excessively.

Parameter Measuring Circuits

Measurement of H_m, H_c, B_m, and B_r is obtained by tracking the H or B signals (e_4 or e_6) and then holding the instantaneous values at the right moment. This is done with a zero crossing detector (ZCD) controlling a sample and hold amplifier. For measurement of H_m and B_m, the ZCD input comes from the bistable multivibrator and operates merely as a sense amplifier.

Zero Crossing Detector

The ZCD is essentially a high gain amplifier with diode output clamping. It was found necessary to cascade two amplifiers A_{14} and A_{15} in order to achieve a sensitivity of better than 1 millivolt and a 1 millisecond response time. The output voltage e_{13} will be about +5.5 volts for positive input voltages as low as .1 millivolt and -5.5 volts for negative input voltages as low as .1 millivolt. The position of switch S_{10} on the front panel determines whether relay L_9 is energized or de-energized when the input voltage to A_{14} goes through zero from negative to positive or from positive to negative. For peak measurements the input to A_{14} comes from the multivibrator output which never goes negative in polarity. This is taken care of by adding one negative diode drop to the multivibrator output e_{10} with diode D_{16}.

Sample and Hold Amplifier

A sample and hold amplifier A_{13} of simple non-inverting design with reed relay switching was chosen for low droop capability while in the hold mode. In the sample mode the contact of relay L_9 is closed and capacitor C_6 charges to the value of the applied input voltage e_4 or e_6, and A_{13} acts as a high impedance unity gain follower. When L_9 opens, the input voltage at that instant is held on C_6 indefinitely except for drift (droop) caused by the leakage resistance of C_6 and input bias current charging from A_{13}. Using an FET input amplifier and a polycarbonate capacitor the resulting drift is about 2×10^{-5} volts per second. In the sample mode the charging time constant $(R_{29}C_6)$ is equal to .3 milliseconds.

Operation of the B-H Meter

The front panel of the B-H meter can be seen in the photograph of figure 15.[18] The procedure for tracing a loop and measureing the key parameters is as follows:

1. The Epstein strips are weighed and the weight in grams is set on the sample weight potentiometer P_1.

---

[18]This photograph shows the control panel prior to two important changes. First the sample weight potentiometer P_2 has been replaced by a greater precision adjustable decade resistance module. Also the labeling on the magnetizing force range switch S_2 is now 1 Oe. and 10 Oe, and the recorder output terminals are appropriately marked 10V/1/10 Oe.

2. The strips are loaded into the Epstein frame and demagnetized with 60 Hz current by rotation of the variac V_1 knob.
3. Method "A"- controlled magnetizing force: the maximum magnetizing force is set to either 1 or 10 oe. on the magnetizing range switch S_2. If an intermediate value of H_m is to be used, then S_2 is set to a variable position and the H_m measurement switch S_3 is depressed so that H_m is displayed on the digital meter. The value of H_m is increased by adjusting potentiometer P_3 during cyclical magnetization until the desired value of H_m is obtained.
4. The centering reset button is depressed and after one cycle the X-Y plotter is activated to trace out a loop.
5. Values of H_m,H_c,B_m and B_r are displayed on the digital meter by depressing the appropriate switch S_3,S_4,S_5 or S_6.
6. Method "B"- controlled induction: The B_m measurement switch S_4 is depressed so that the peak induction is displayed on the digital meter. The magnetizing range switch S_2 is set to a variable position and P_3 is adjusted during cyclical magnetization until the desired value of B_m is obtained. The centering reset button is used at least once to center the loop.
7. Same as step 4.
8. Same as step 5

Loop cycle rate can be varied by adjusting potentiometer P_2. Both the centering circuit and dB/dt feedback are cut out by opening switch S_8. Display of either polarity of the key parameters is made possible by operation of switch S_{10}.

CHAPTER III

SUMMARY

Discussion of Measurement Errors

B and H Computing Accuracy

In general, the gains of A_1, A_6 and A_7 will affect the precision to which the specimen induction is computed from the B-coil induced voltage. However, adjustment of R_{12} permits trimming of the overall gain of the B computing circuit to an accuracy dependent on the method of calibration. The most direct calibration method consists of applying a known constant voltage for a known time period to the input of A_1, and then R_{12} can be adjusted to obtain the calculated value of e_4 from equation (21). Using this method the B computing circuit has been calibrated to an accuracy of .1%. The inaccuracy or non-linearity of potentiometer P_1 introduces gain errors for different weight settings of about .01%. The centering circuit must be bypassed for the gain calibration, but when it is used in loop tracing the symetry of peak induction values can be directly observed to be within .1% of peak values. The total error in computing B (e_4), including gain error, P_1 error, and centering error is then .21%.

The accuracy of magnetizing force computation is determined by the precision of the shunt resistor (R_{13} or R_{14}) and the feedback resistors (R_{15},R_{16},R_{17},R_{18}) of A_8. These resistors are all .02% tolerance wirewound types and the gain of A_8 has been verified to be within

.1% of the required value using a standard resistor and precision voltmeter. No adjustment for gain trimming is provided since long term gain drift should be less than .05%. The output offset voltage of A_7 can be trimmed to less than 50 microvolts and is negligible.

Sampling Errors

In this section the errors associated with sampling the B and H signals (e_4 and e_6) for display on the digital panel meter will be analyzed. For example, when a measurement of coercive force H_c is made, the zero crossing detector senses the instant when the induction (e_4) is zero and causes the sample and hold relay L_9 to open so that the value of H (e_6) at that instant is held for display on the digital meter. However, there is a time lag between the instant of B=0 and the opening of relay L_9, caused by the overdrive or sensitivity requirement of the ZCD and the release time of L_9. Also, the actual value of e_4 when B=0 may not be zero if loop centering is not perfect.

The sampling errors will not be identical for measurement of each parameter since they are dependent on the rate at which the signals are changing. Thus general expressions will be developed for the sampling errors of each measurement separately, and the following notation will be used:

V_{H-Hm} = rate of change of H signal at H_m in volts/second

V_{B-Bm} = rate of change of B signal at B_m in volts/second

V_{H-Hc} = rate of change of H signal at H_c in volts/second

V_{H-Br} = rate of change of H signal at B_r in volts/second

V_{B-Br} = rate of change of B signal at B_r in volts/second

V_{B-Hc} = rate of change of B signal at H_c in volts/second

H_m Sampling Error

When the peak magnetizing current is reached the bistable multivibrator output changes abruptly and is sensed by the ZCD. The ZCD response time will be less than 100 microseconds because of the relatively large multivibrator output swing, but the release time of relay L_9 may be 500 microseconds or more. Ignoring the ZCD response time, the release time of L_9 will be called t_r seconds. With the H signal changing at the rate of V_{H-Hm} volts/second, the sampling error is:

$$H_m \text{ error} = (V_{H-Hm})t_r \text{ volts} \tag{45}$$

B_m Sampling Error

Again the response time of the ZCD can be neglected, and the sampling error caused by the release time of L_9 is:

$$B_m \text{ error} = (V_{B-Bm})t_r \text{ volts} \tag{46}$$

H_c Sampling Error

In the case of the H_m and B_m measurements the input voltage to the ZCD undergoes an almost instantaneous polarity reversal of relatively large magnitude. For this reason, the sensitivity and input voltage offset of the ZCD amplifier is not critical. This is not the case for measurement of H_c and B_r where the input to the ZCD goes through zero relatively slowly. The ZCD requires some small finite voltage called overdrive in order to change state. This overdrive requirement will be included with input offset error and called V_{od}. Again let t_r seconds be required for the relay L_9 to open. Also let the B signal zero error (centering circuit imperfect) be designated as V_{bo} volts. In order to provide the V_{od} volts overdrive, a time period of V_{od}/V_{B-Hc} seconds will be required for the B singal to increase from 0 to V_{od} volts. In a similar manner, the B signal zero error is equivalent to a timing error of V_{bo}/V_{B-Hc} seconds. The total error in H_c sampling will be equal to the rate of change of the H signal times the total equivalent timing error, or:

$$H_c \text{ error} = V_{H-Hc}\left[\frac{V_{od} \pm V_{bo}}{V_{B-Hc}} + t_r\right] \text{ volts} \qquad (47)$$

<u>B_r Sampling Error</u>

Again let the ZCD overdrive requirement be V_{od} volts and allow t_r seconds for L_9 release. There is no error in the H signal at H=0 because the zero offset of the differential amplifier A_8 is negligible. Thus the sampling error in B_r measurement is:

$$B_r \text{ error} = V_{B-Br}\left[\frac{V_{od}}{V_{H-Br}} + t_r\right] \text{ volts} \qquad (48)$$

It is clear from equations (45) to (48) that it is desireable to keep t_r as small as possible. Very fast switching times could be achieved with electronic switches such as MOSFETs, but at the penalty of increased leakage current or voltage offsets, and the speed improvement is not actually necessary. Slowing down the rate of loop tracing will also reduce the sampling errors, but with only partial effect in H_c and B_r measurement because of the overdrive requirement of the ZCD. This becomes clear when it is recognized that the ratios V_{H-Hc}/V_{B-Hc} and V_{B-Br}/V_{H-Br} from equations (47) and (48) are constant regardless of sweep rate; these ratios are proportional to the differential permeability and its reciprocal and vary from point to point on the hysteresis loop, but do not vary with sweep rate.

When equations (45) through (48) are evaluated with typical values the predicted errors vary between .1 and 1 millivolt, but it has not been possible to experimentally verify these predicted error limits. However, the digitally measured values of H_m,H_c,B_m and B_r agree with the values read from the hysteresis loop traces within the accuracy of the X-Y plotter.

Examples of Performance

Figures 16 through 19 are examples of hysteresis loops and measurements made with the B-H meter. Both positive and negative polarity values of H_m,H_c,B_m, and B_r as read from the digital panel meter are included in the upper left corner of the loop figures. Figures 16 and 17 were made with a 20 strip sample of 11 mil silicon steel at peak magnetizing forces of 1 and 10 Oe. respectively. In figure 18 a series of loops of increasing peak magnetizing force was made with the same 11 mil sample. Figure 19 shows two loops made with a 16 strip sample of 25 mil non-oriented silicon steel at peak magnetizing forces of 1 and 10 Oe.. Finally, the excellent drift stability of the flux integrator can be seen from the 10 Oe. loop of figure 19; it is actually a multiple trace with a loop cycle time of 40 seconds, and was run for a total of 10 minutes or 15 loops.

Final Discussion

The hysteresigraph which has been described here provides accurate measurements of magnetization characteristics of electrical steels without resorting to complicated test procedures. Although this instrument is tailored for Epstein frame testing, the signal conditioning concepts described in the design analysis can provide a basis for designing instruments for other permeameters or excitation and field measurement methods.

The discussion of accuracy given earlier was concerned only with the errors associated with the electronics of the B-H meter. However, the overall accuracy of magnetization measurements is largely determined by the validity of equation (22) in computing the magnetizing force from the exciting current of the Epstein frame. It is known that the effective magnetic path length is not constant and errors of several per cent can be possible under the assumption of any one value of L_c[17]. The effect of air gaps at the joints is readily demonstrated with the B-H meter by noting changes in B_r when the corners of the laminations are clamped. To a lesser extent, the material induction determination is complicated by imperfect air flux compensation, especially at large magnetizing forces. The most accurate magnetization data can be provided by properly made ring core or toroidal samples when this is practical, but Epstein frame testing is well suited to comparative studies of electrical steels. Regardless of the geometry of the sample and magnetic coupling circuit, comparative studies of magnetization properties bene-

---

[17] ASTM 371-S1, p.20.

fit from stable instrumentation as is the case with this B-H meter.

A number of modifications are being worked out to further improve the utility and accuracy of the B-H meter in its present form. Some are minor such as substituting a fast comparator for A_{14} and A_{15}. Major changes will include extension of the peak magnetizing force to 100 Oe. for the Epstein frame, or a peak current of 10 amperes for ring core testing; with adjustable scaling for calibrated ring core testing.

APPENDIX FIGURES

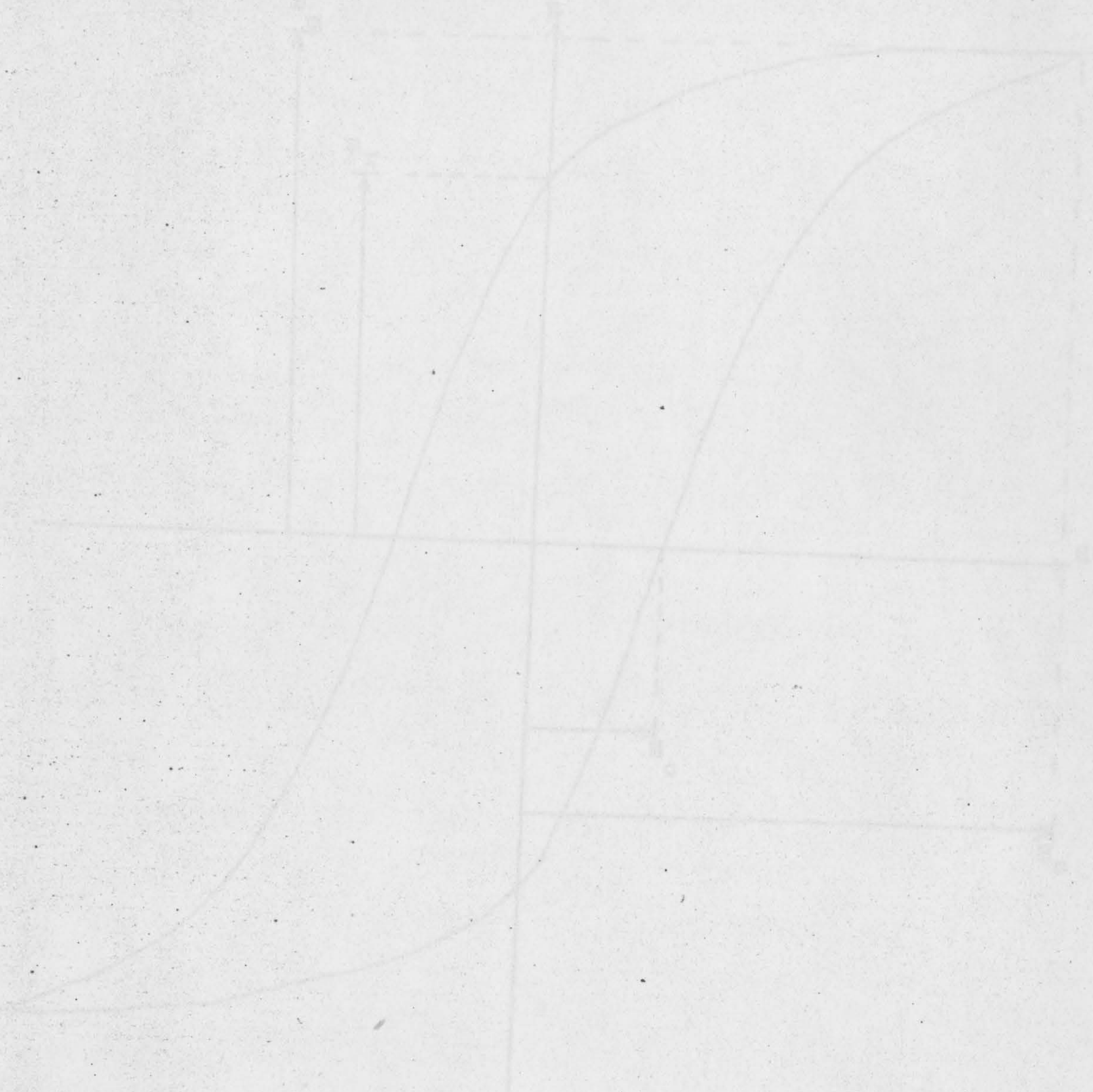

FIGURE 1 Typical B-H Loop

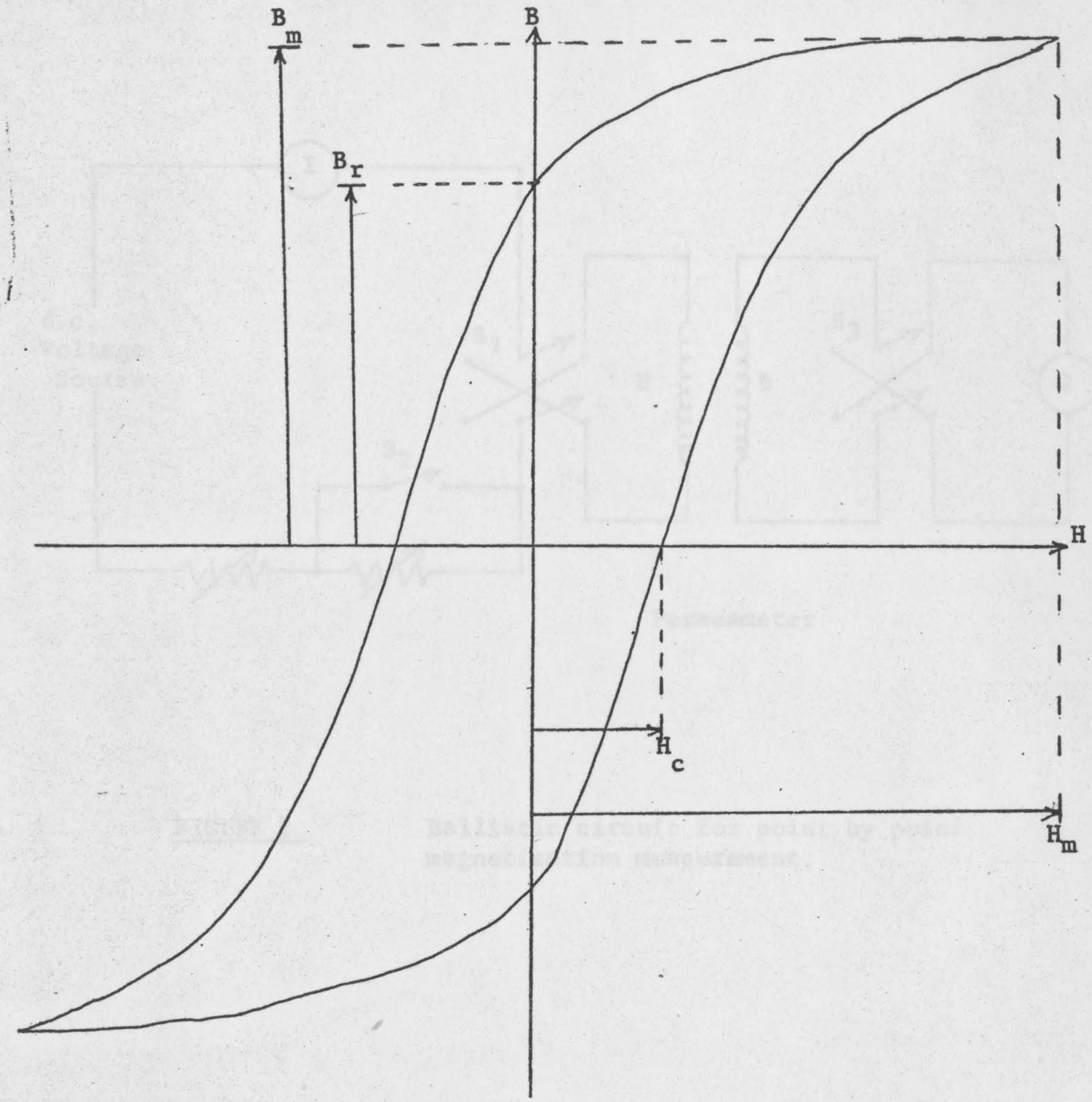

FIGURE 1 Typical B-H Loop

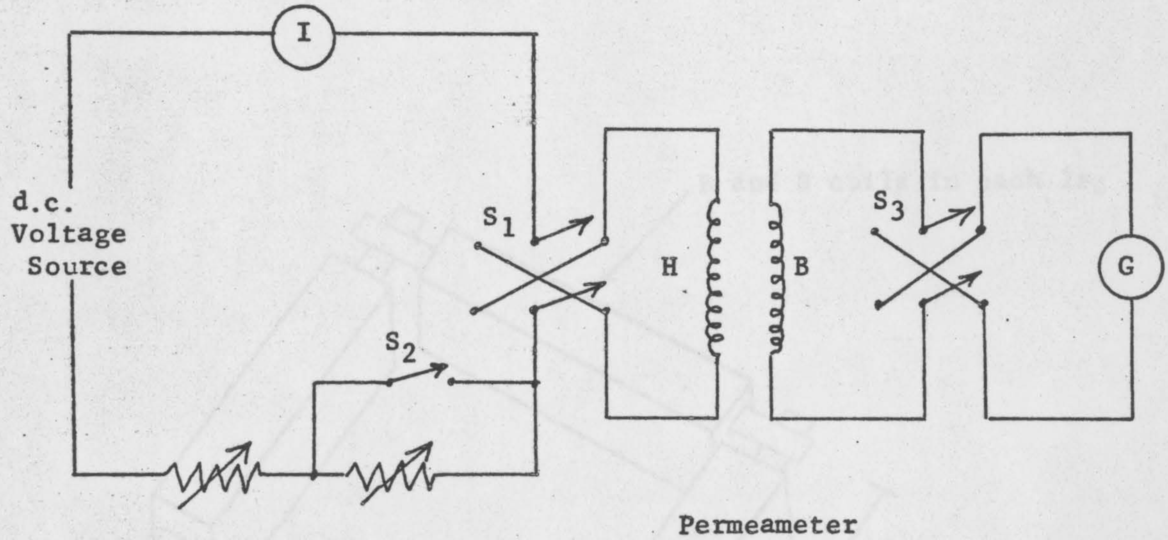

FIGURE 2 Ballistic circuit for point by point magnetization measurement.

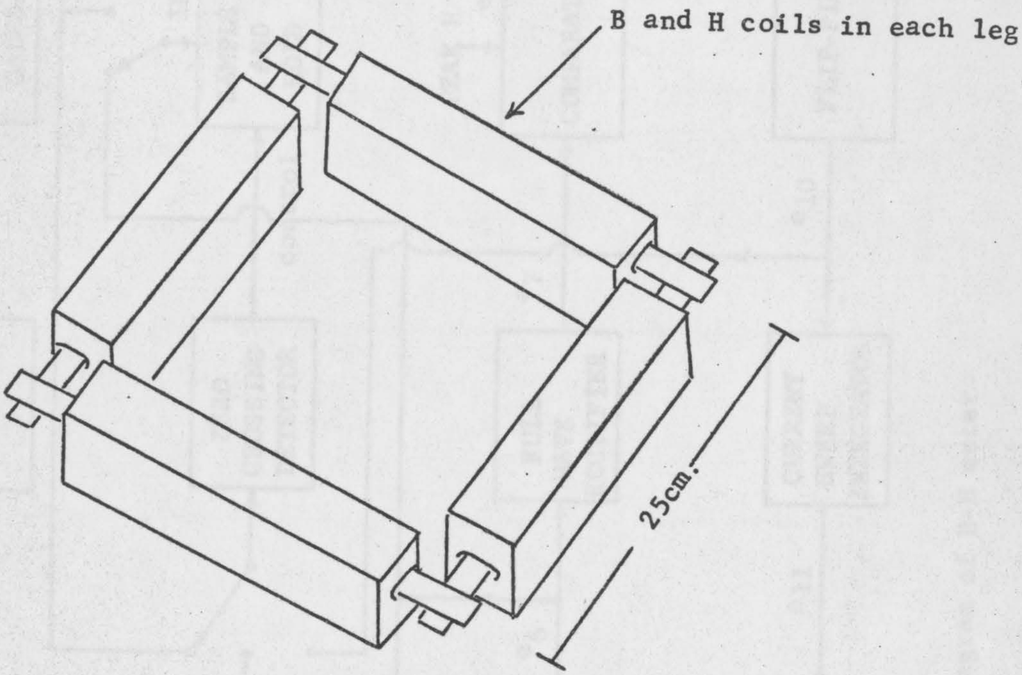

FIGURE 3 Epstein frame construction

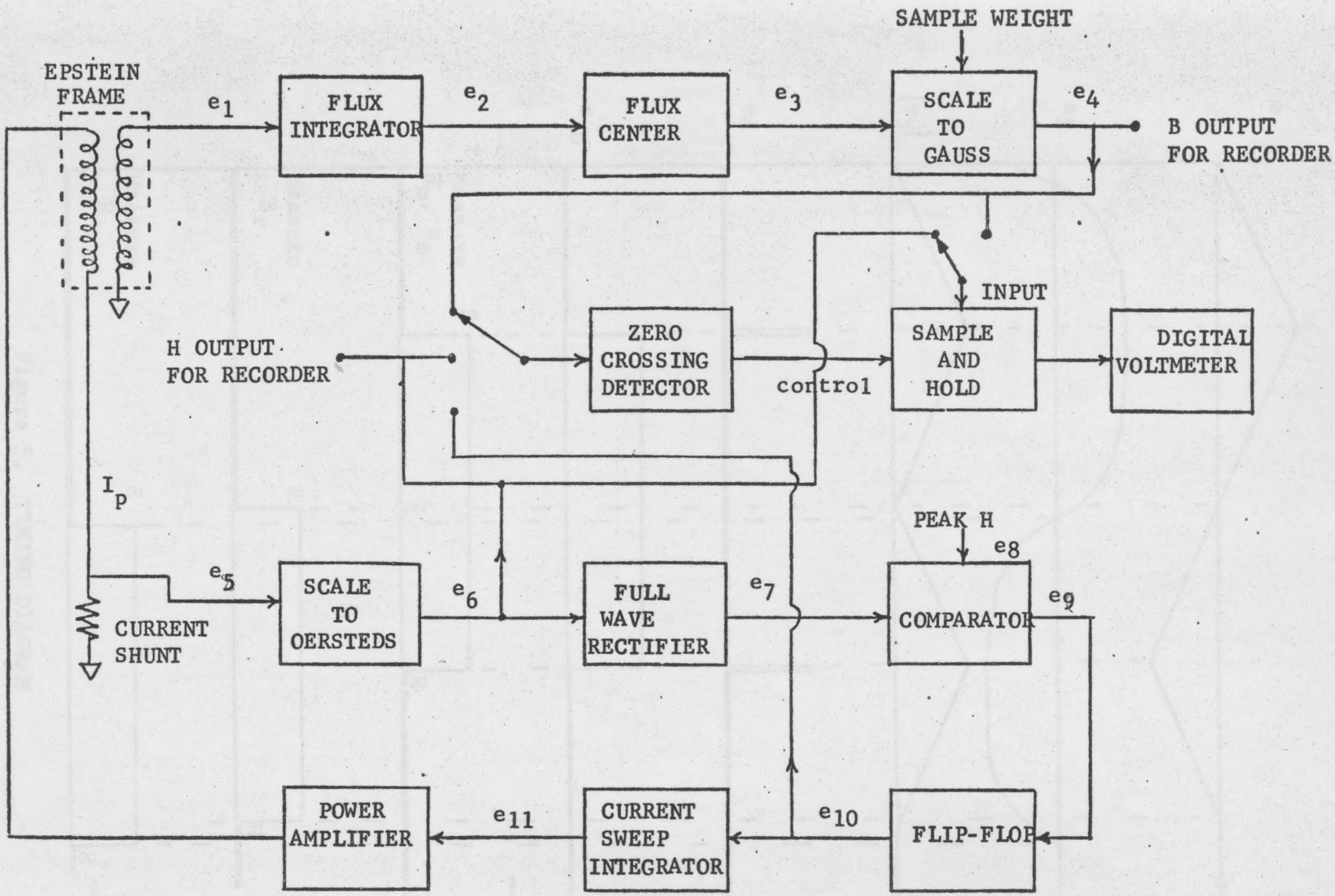

FIGURE 4 Block diagram of B-H meter

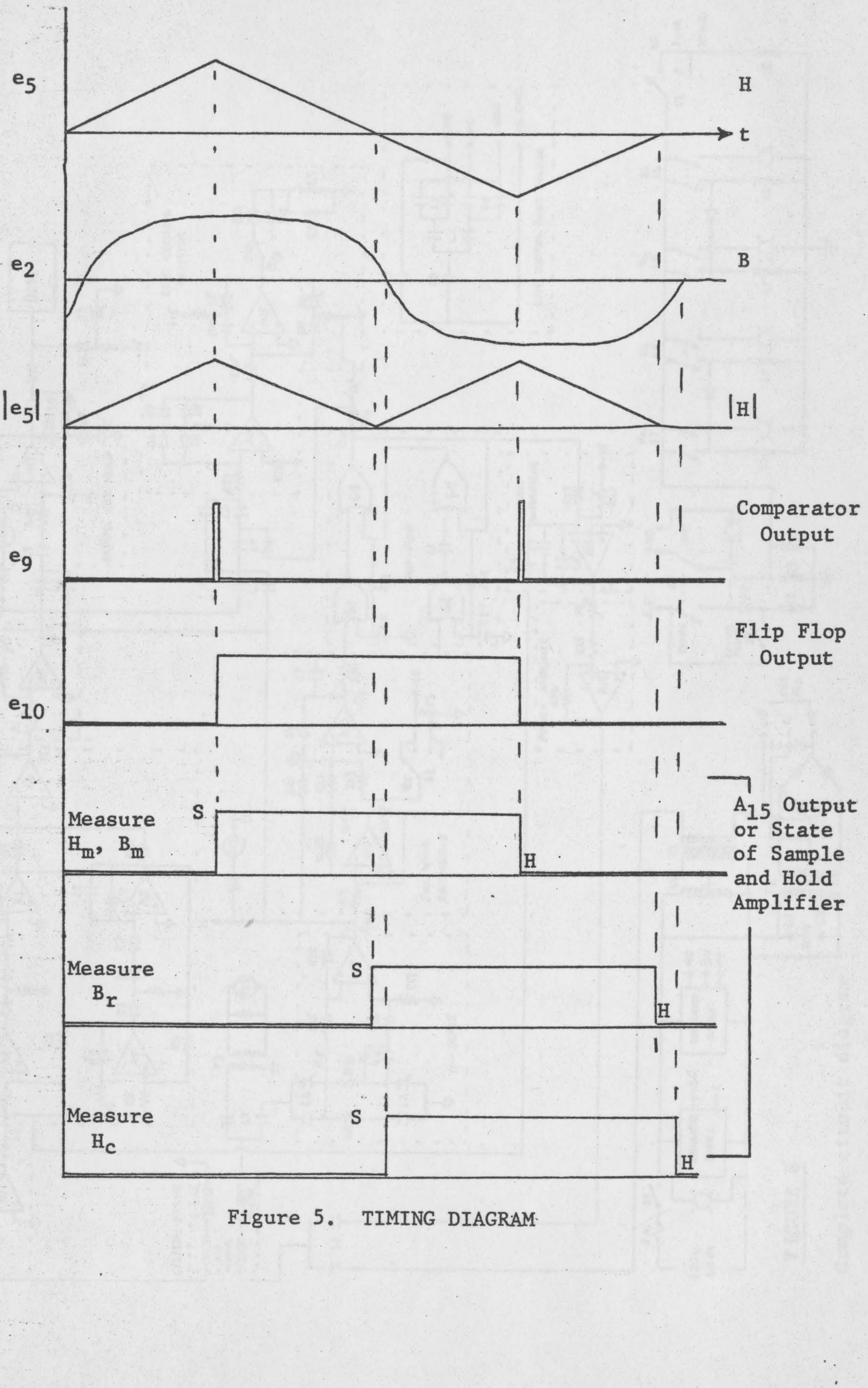

Figure 5. TIMING DIAGRAM

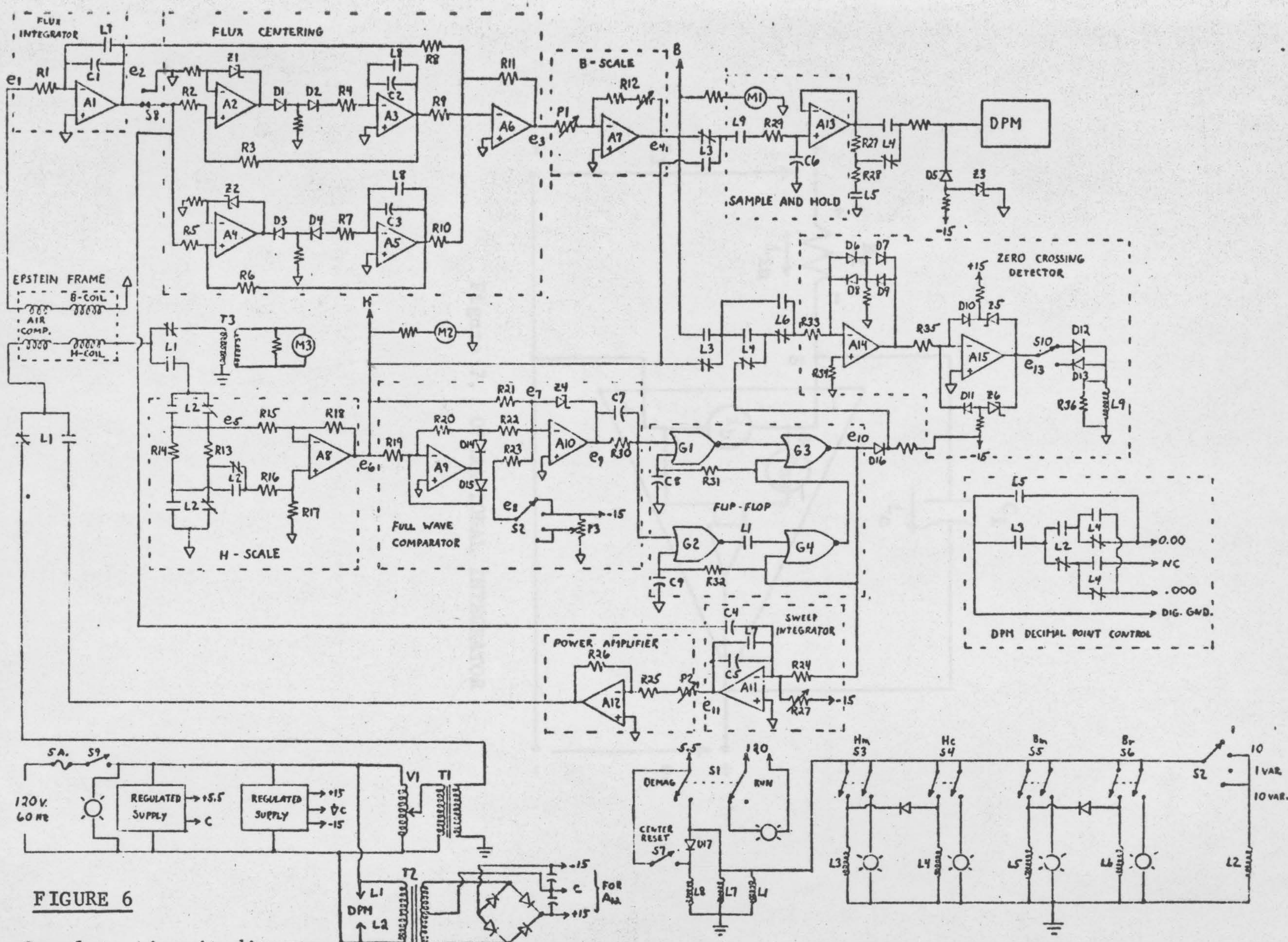

FIGURE 6

Complete circuit diagram

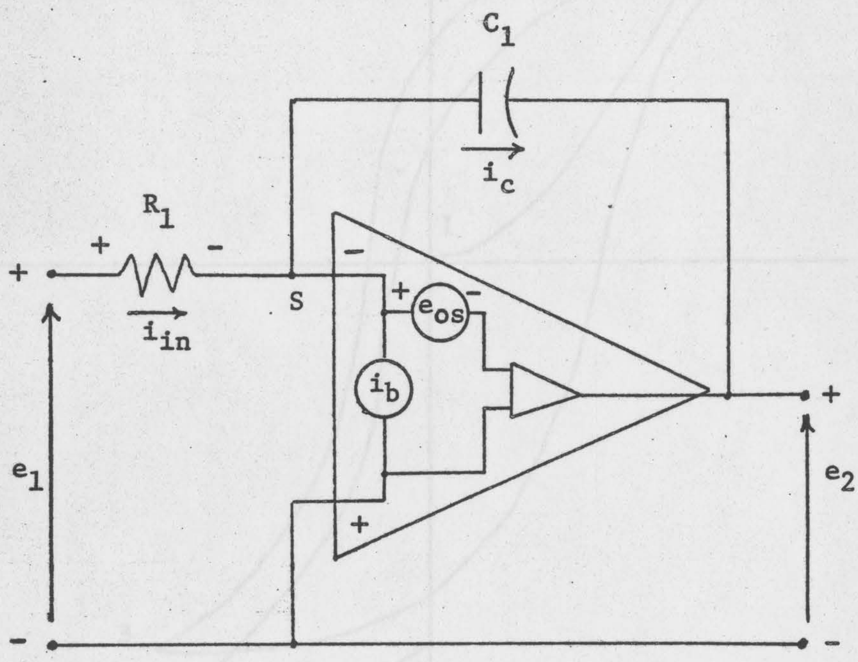

Figure 7. OPERATIONAL INTEGRATOR

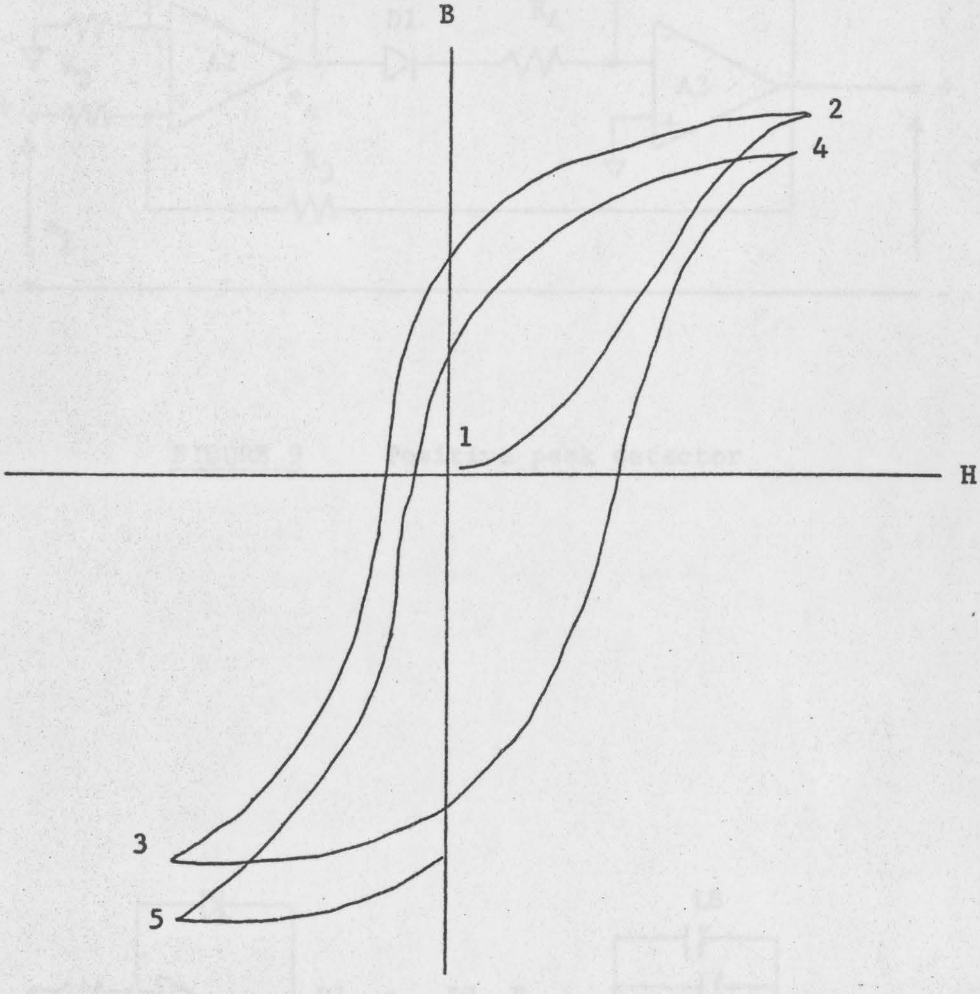

FIGURE 8 Loop shift starting from demagnetized state

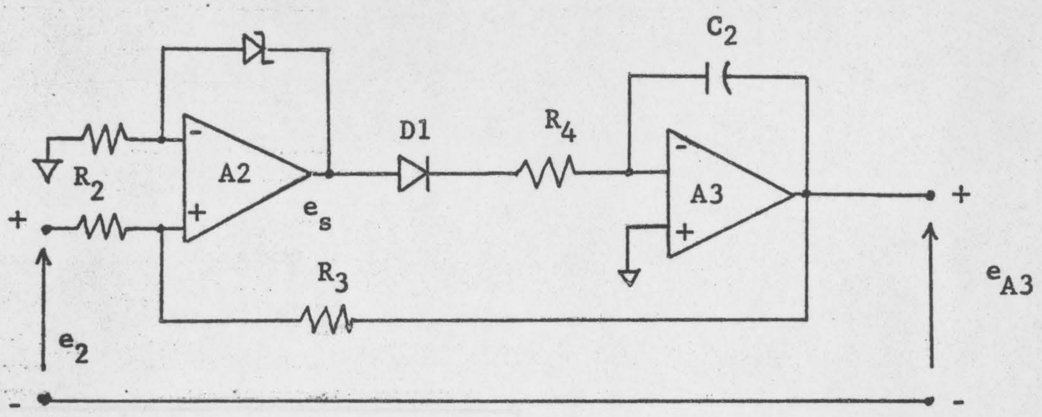

FIGURE 9 Positive peak detector

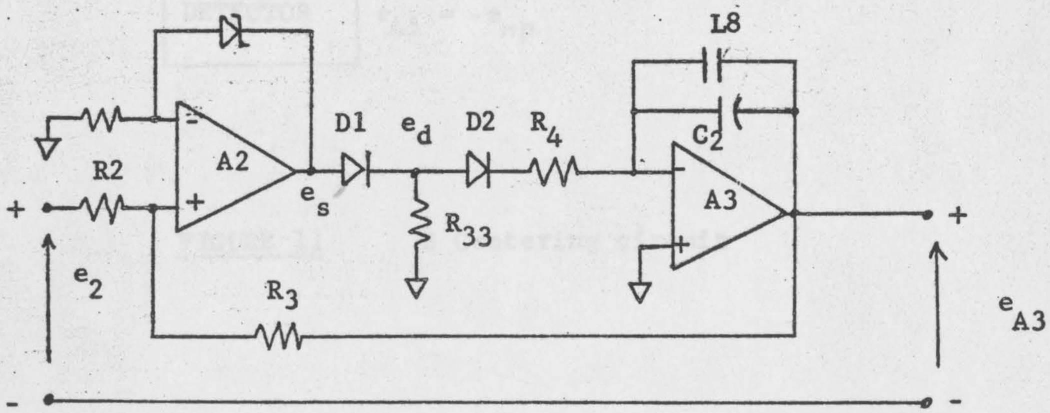

FIGURE 10 Positive peak detector with high diode isolation

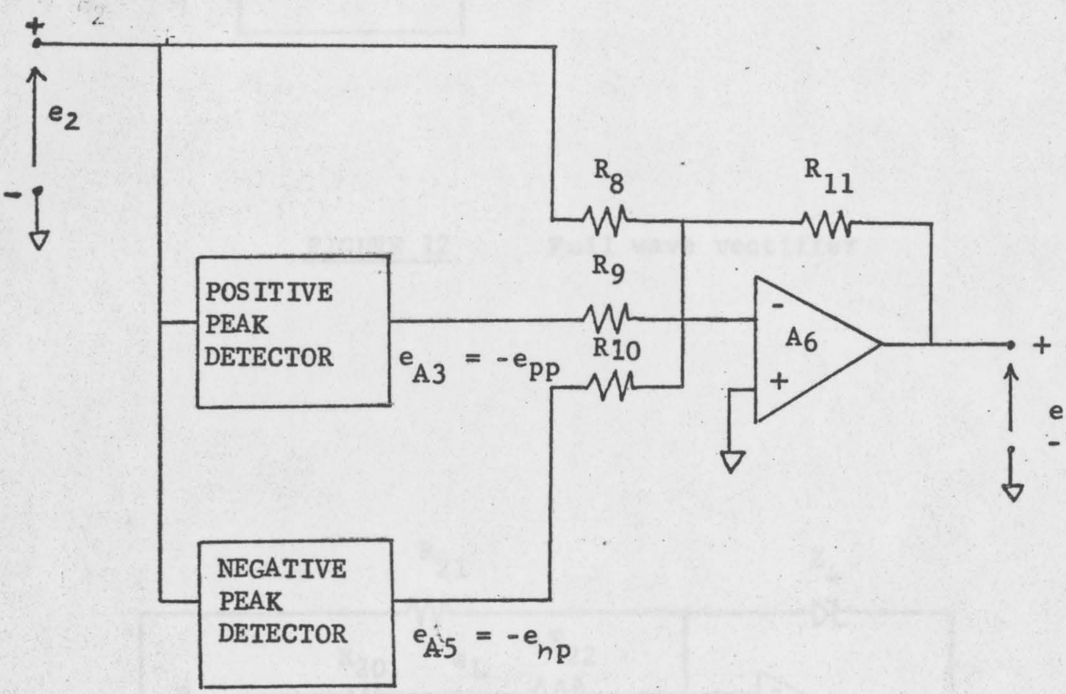

FIGURE 11 B Centering circuit

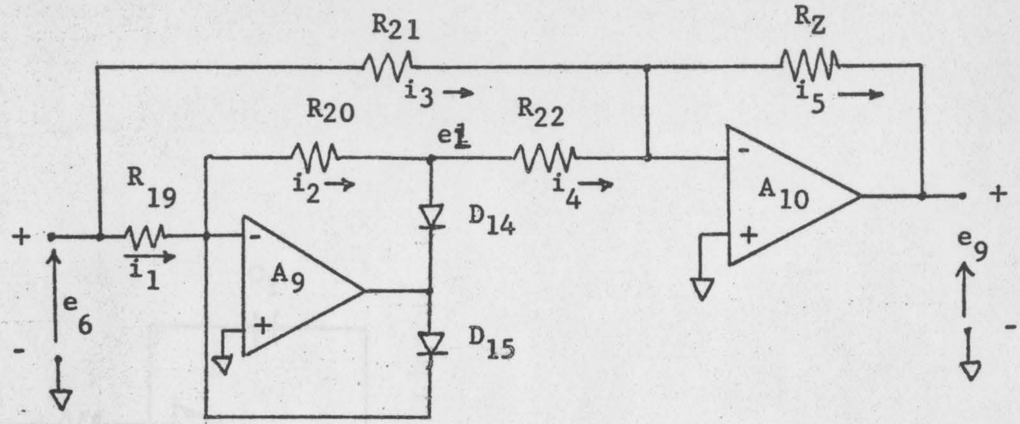

FIGURE 12 Full wave rectifier

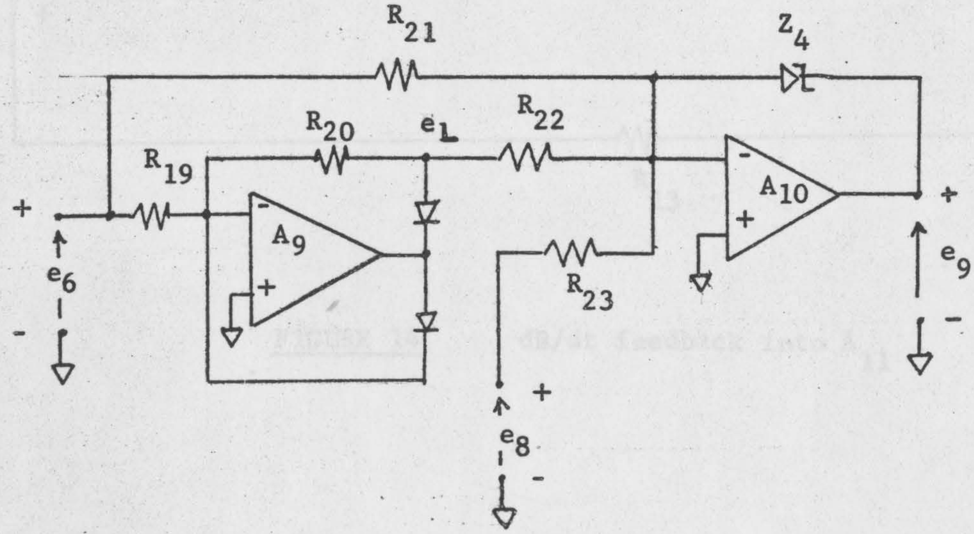

FIGURE 13 Full wave comparator

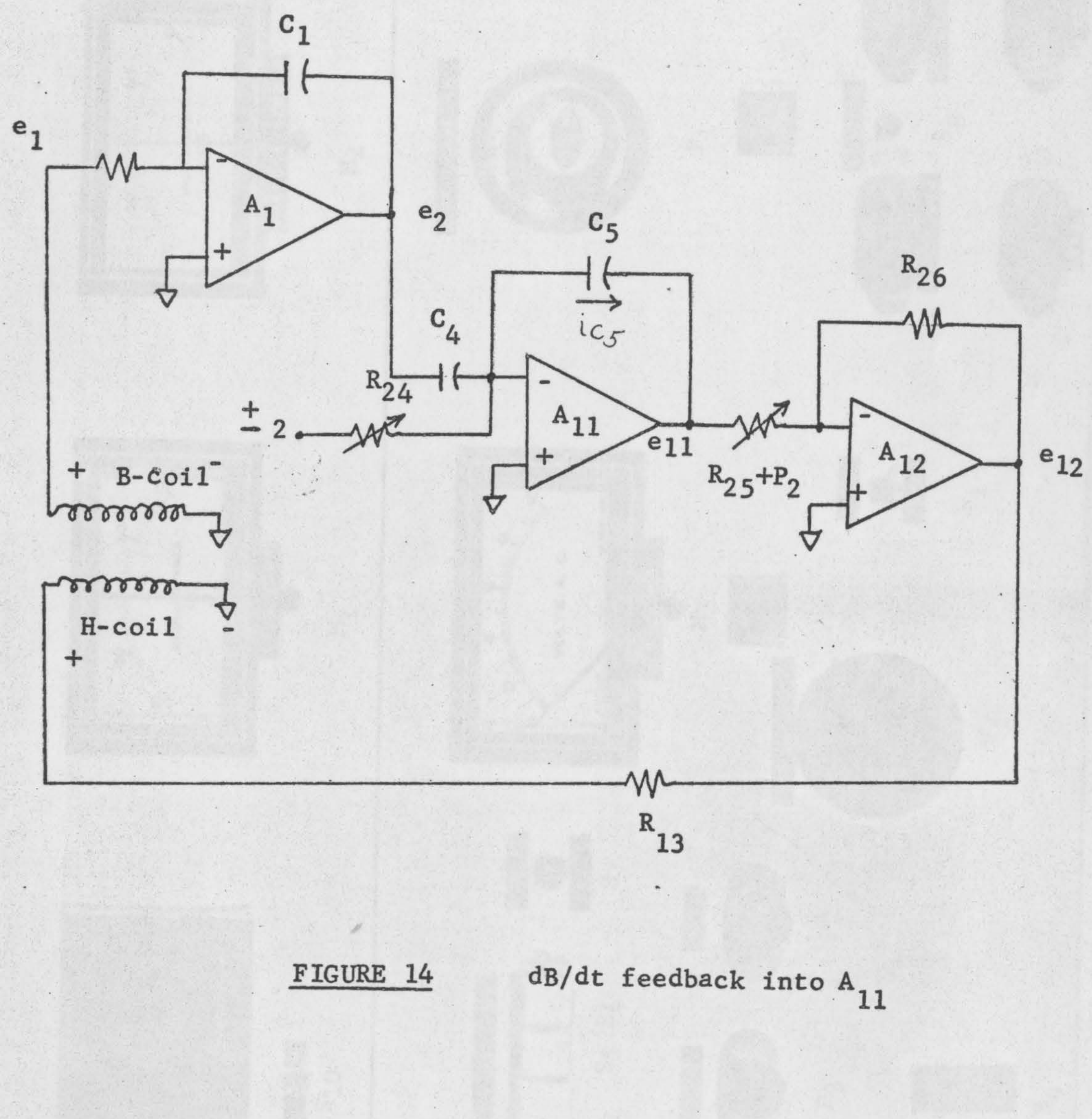

<u>FIGURE 14</u> dB/dt feedback into A_{11}

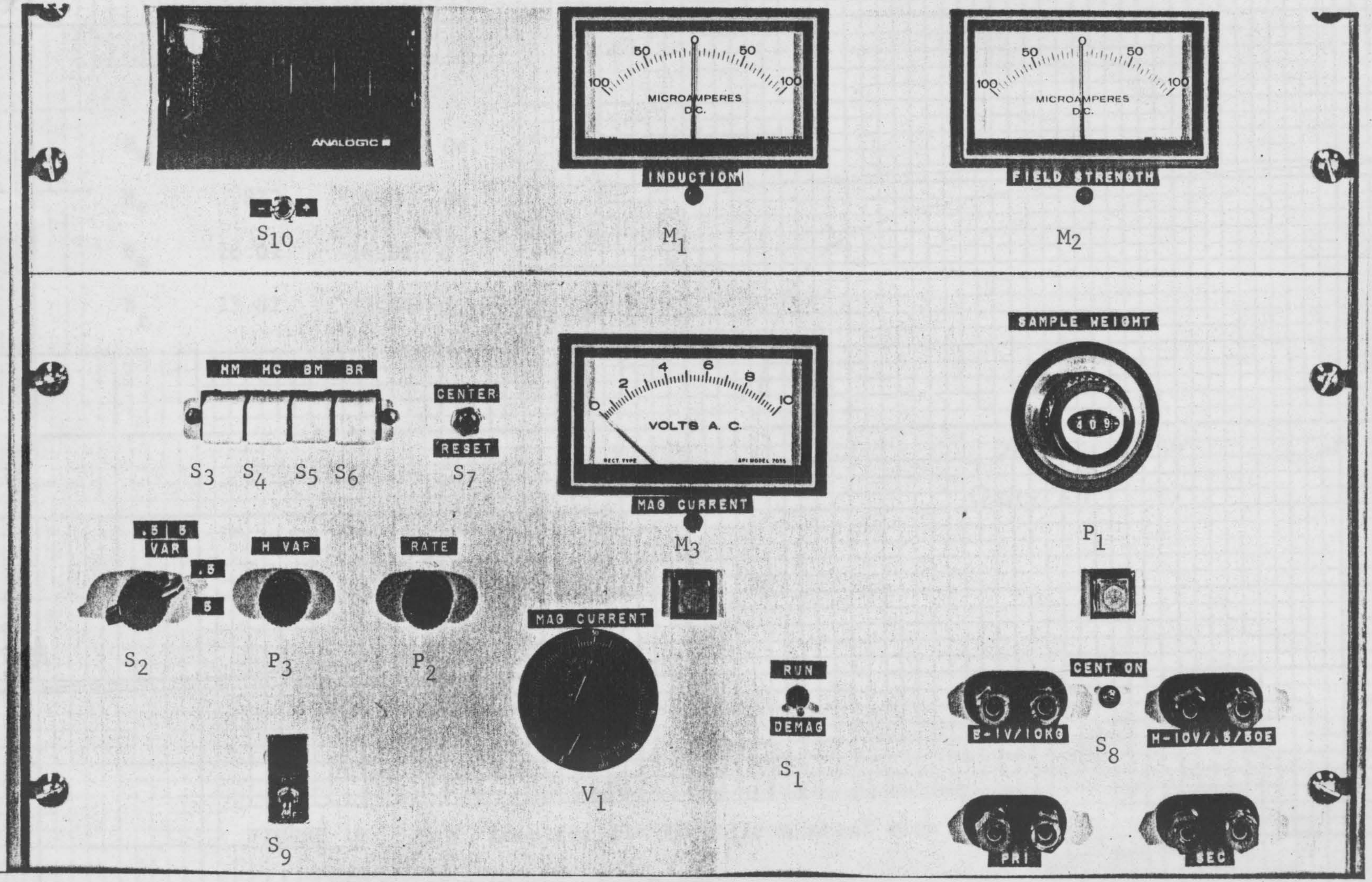

FIGURE 15 Front panel of B-H meter

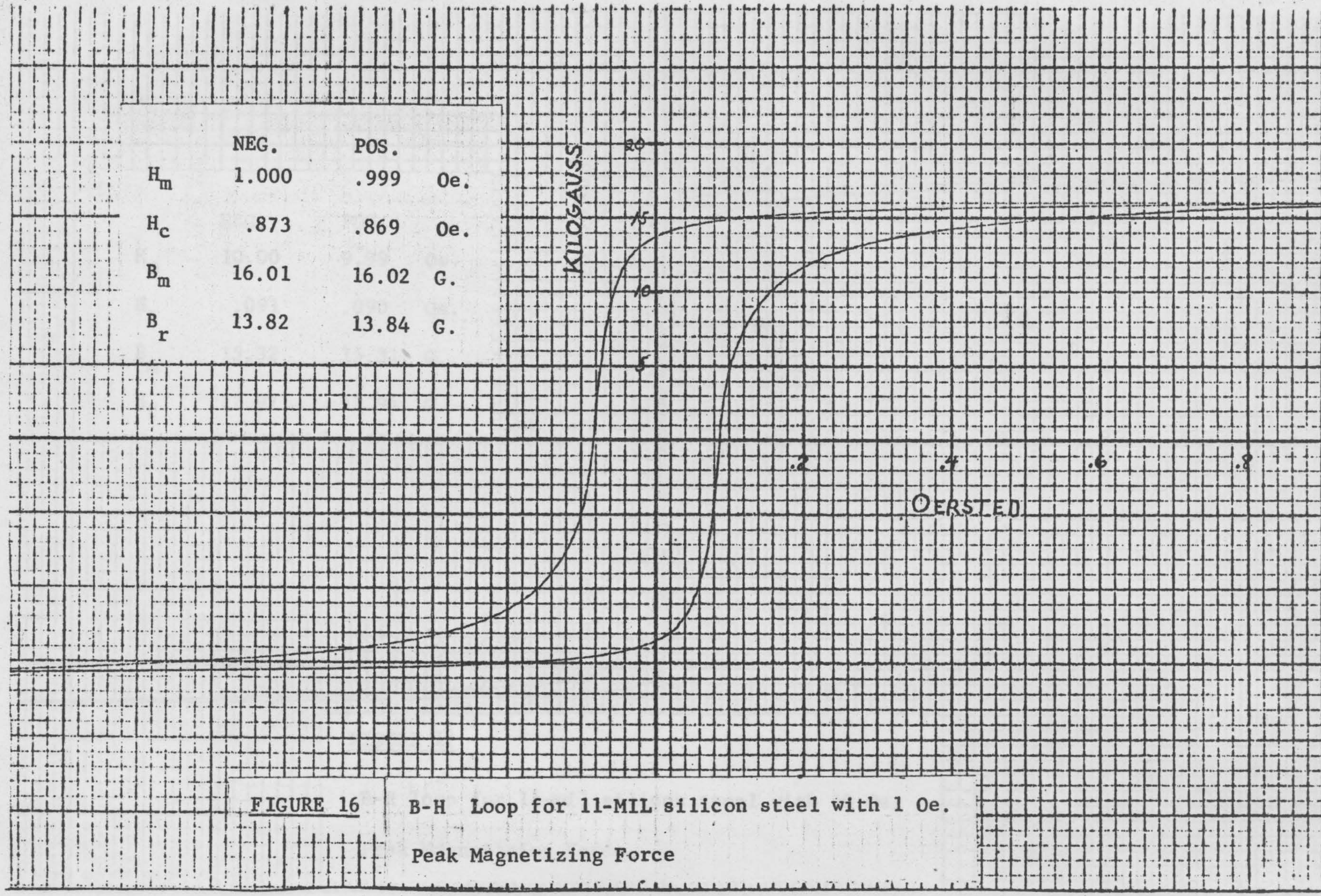

FIGURE 16 B-H Loop for 11-MIL silicon steel with 1 Oe. Peak Magnetizing Force

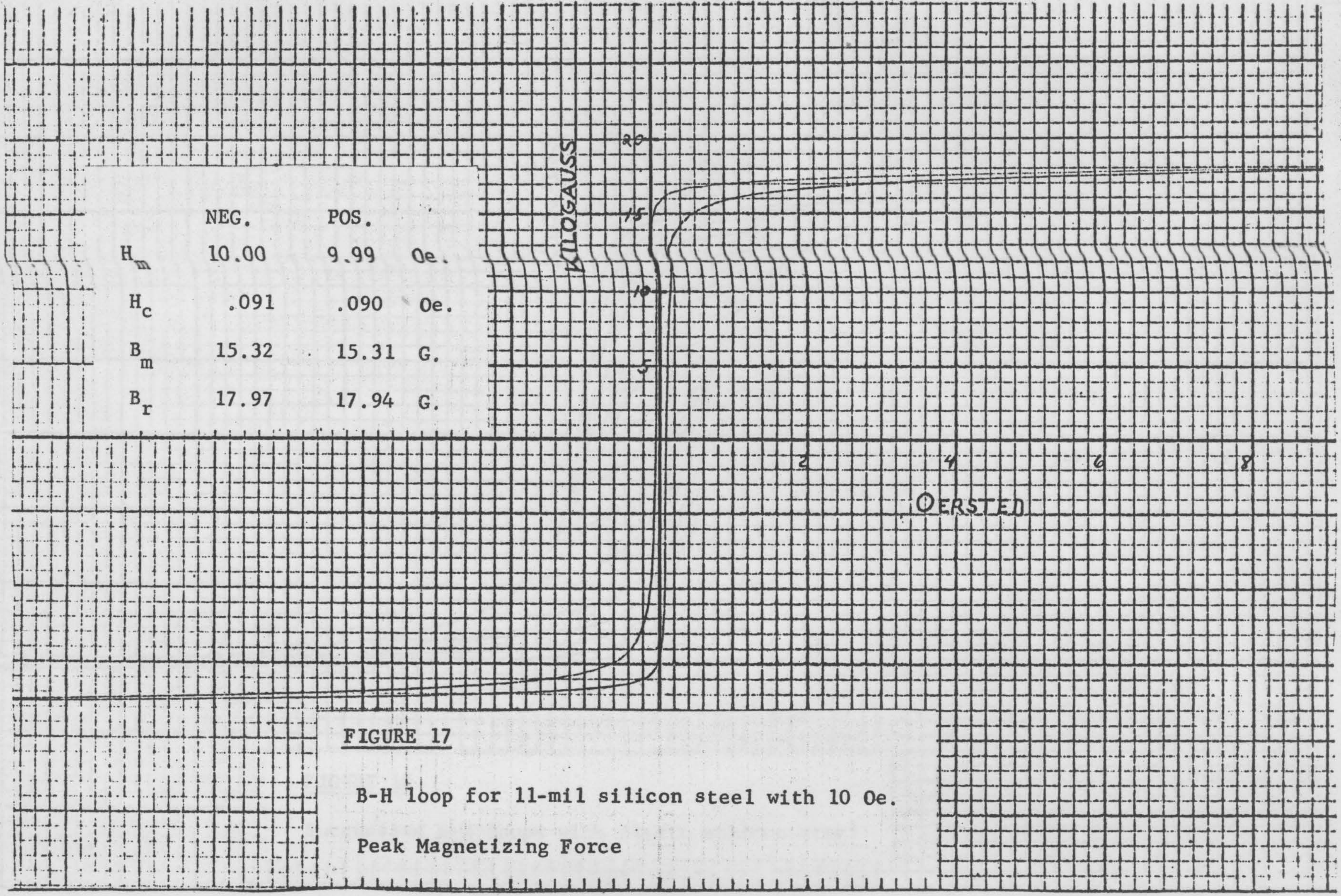

	NEG.	POS.	
H_m	10.00	9.99	Oe.
H_c	.091	.090	Oe.
B_m	15.32	15.31	G.
B_r	17.97	17.94	G.

FIGURE 17

B-H loop for 11-mil silicon steel with 10 Oe.

Peak Magnetizing Force

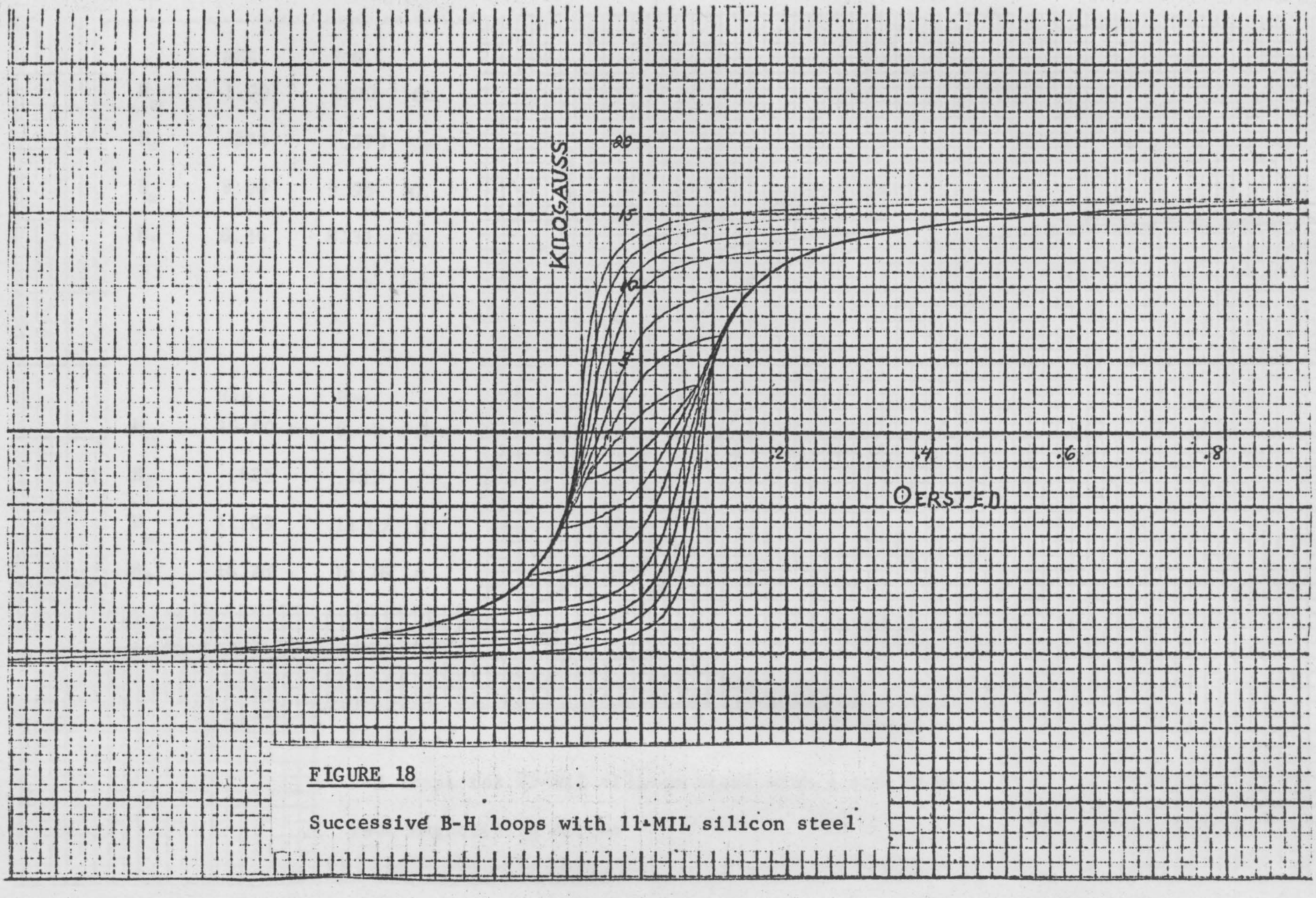

FIGURE 18

Successive B-H loops with 11-MIL silicon steel

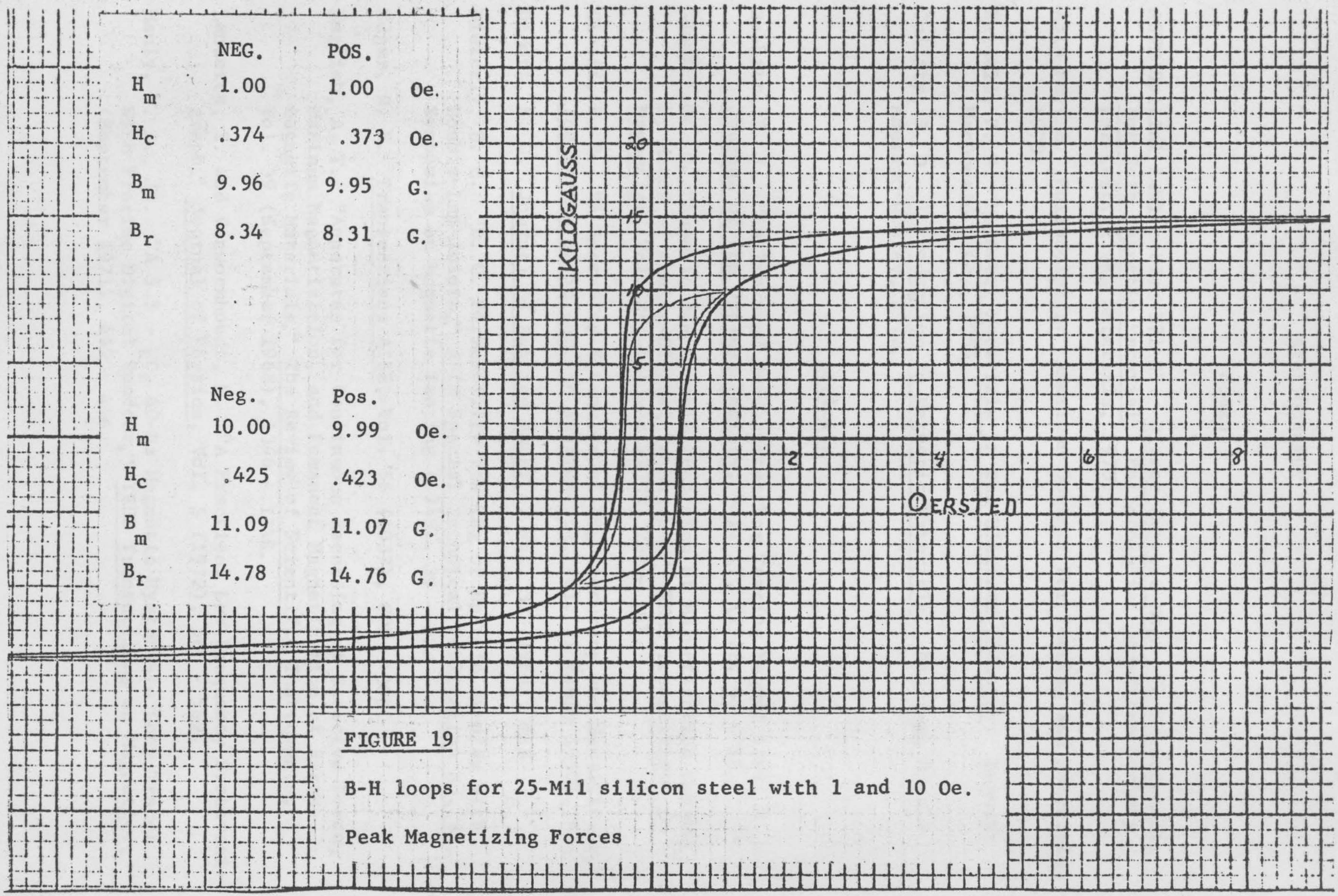

	NEG.	POS.	
H_m	1.00	1.00	Oe.
H_c	.374	.373	Oe.
B_m	9.96	9.95	G.
B_r	8.34	8.31	G.

	Neg.	Pos.	
H_m	10.00	9.99	Oe.
H_c	.425	.423	Oe.
B_m	11.09	11.07	G.
B_r	14.78	14.76	G.

FIGURE 19

B-H loops for 25-Mil silicon steel with 1 and 10 Oe.

Peak Magnetizing Forces

BIBLIOGRAPHY

Books

ASTM Special Publication 371-S1. Direct Current Magnetic Measurements For Soft Magnetic Material. Philadelphia: American Society For Testing and Materials, 1970.

ASTM Part 8. Philadelphia: American Society For Testing and Materials, 1973.

Bardell, P. R. Magnetic Materials in the Electric Industry. London: MacDonald & Co., 1955.

Cullity, B. D. Introduction to Magnetic Materials. Reading, Mass.: Addison-Wesley, 1972.

Articles

Babbitt, B. J. "An Improved Permeameter For Testing Magnet Steel," Journal of the Optical Society, Vol. 17, (1928), 47 - 58.

Capptuller, H. "Numeric and Graphic Recording of Magnetization Curves by Means of Analog-Digital Techniques," IEEE Transactions on Magnetics, Vol. Mag-6 (June 1970), 263 - 265.

Cioffi, P. P. "A Recording Fluxmeter of High Accuracy and Sensitivity," The Review of Scientific Instruments, Vol. 21 (July 1950), 624 - 628.

DeMott, E. G. Journal of Applied Physics, Vol. 37 (1966), 118

Dieterly, D. C. "D. C. Permeability Testing of Epstein Samples With Double-Lap Joints," ASTM Special Technical Publication No. 85, Symposium on Magnetic Testing (1949). 39 - 62.

Edgar, R. F. Transactions AIEE, Vol. 56 (1937), 805 - 809.

English, A. T. "Apparatus for Continuous Recording of Coercive Force, Maximum Magnetization, and Remanent Magnetization of Ferromagnetic Materials," The Review of Scientific Instruments, Vol. 39 (September 1968), 1346 - 1348.

Lenaerts, I. and Vanwormhoudt, M. "A Practical Low Frequency Hysteresigraph," Journal of Physics, Vol. 5 (1972), 560 - 562.

Manly, W. A., Jr. "A 5.5 - $_{K}O_{E}$ 60-Hz Magnetic Hysteresis Loop Tracer With Precise Digital Readout," IEEE Transactions on Magnetics, (September 1971), 442 - 446.

Mazzetti, P. and Soardo, P. "Electronic Hystersigraph Holds dB/dt Constant;" The Review of Scientific Instruments, Vol. 37 (May 1966), 548 - 552.

Sanford, R. L. "Performance of Fahy Simplex Permeameter," Journal of Research, National Bureau of Standards, Vol. 4 (May 1930), 703 - 707.

Smith, B. D. "A New Full Range Permeameter;" General Electric Review, Vol. 38 No. 11 (November 1935), 520 - 522.